

**An-Najah National University**

**Faculty of Graduate Studies**

**Characterization of Dissolved Organic Matter in  
Wadi Al-Badan using Fourier Transform Infrared  
Microspectroscopy at SESAME**

**By**

**Amal Atari**

**Supervisor**

**Dr. Ahmed Bassalat**

**Co-Supervisor**

**Dr. Sameer Shadeed**

**This Thesis is Submitted in Partial Fulfillment of the Requirements for  
the Degree of Master of physics, Faculty of Graduate Studies, An-Najah  
National University, Nablus, Palestine.**

**2019**

**Characterization of Dissolved Organic Matter in Wadi  
Al-Badan using Fourier Transform Infrared  
Microspectroscopy at SESAME**

**By  
Amal Atari**

**This Thesis was defended successfully on 15/5/2019, and approved by:**

**Defense committee members**

**Signature**

- |  |       |
|--|-------|
| <b>– Dr. Ahmed Bassalat/ Supervisor</b>        | ..... |
| <b>– Dr. Sameer Shadeed/ Co-Supervisor</b>     | ..... |
| <b>– Dr. Hadil Abualrob/ Internal Examiner</b> | ..... |
| <b>– Dr. Hussein Shanak/ External Examiner</b> | ..... |

## **Acknowledgment**

I would like to thank both of my supervisor Dr. Ahmed Bassalat and Dr. Sameer Shadeed for their help, advises, efforts, and encouragement throughout this thesis. Special thanks also for Dr. Ahmed Bassalat and Dr. Hadil Abualrob for giving me the strength and patience to complete this research as well as supporting me to attend various conferences and several meeting.

Many thank to ICTP and SESAME for offering my master fellowship at SESAME. Special thanks for Dr. Gihan Kamel for all comments and discussion, in particular during my work at SESAME.

Thanks to WESI library staff for the help and advises they offered though the sampling preparation.

My deepest love and appreciation to my mother, father, brothers, sister, and my husband for their support, encouragement and care to complete this thesis.

Thank you all, and thanks for everybody contributed to the success of this thesis, meanwhile expressing my apologies for being unable to mention their names.

**الإقرار**

انا الموقع ادناه مقدم الرسالة التي تحمل عنوان:

**Characterization of Dissolved Organic Matter in Wadi Al-Badan using Fourier Transform Infrared Microspectroscopy at SESAME**

أقر بان ما اشتملت عليه هذه الرسالة انما هو نتاج جهدي الخاص باستثناء ما تمت الإشارة اليه حيث ورد وان هذه الرسالة ككل او اي جزء منها لم يقدم من قبل لاي درجة او بحث علمي او بحثي لدى اي مؤسسة تعليمية او بحثية اخرى.

**Declaration**

The work provided in this thesis, unless otherwise referenced, is the researcher's own work, and has not been submitted elsewhere for any other degree or qualification.

**Student Name****اسم الطالب:****Signature****التوقيع:****Data****التاريخ**

## List of Contents

|   |     |
|---|-----|
| Acknowledgment .....  | III |
| Declaration .....   | IV  |
| List of Contents .....  | V   |
| List of Figures .....   | VII |
| List of Tables.....   | IX  |
| Abstract .....  | X   |
| Chapter One Introduction.....   | 2   |
| 1.1 General Background .....  | 2   |
| 1.2 Research Problem .....  | 3   |
| 1.3 Research Objective .....  | 4   |
| 1.4 Thesis Outline.....   | 4   |
| Chapter Two Application of Synchrotron Radiation .....  | 7   |
| 2.1 Synchrotron-light for Experimental Science and Applications in<br>the Middle East (SESAME)..... | 9   |
| 2.1.1 Storage Ring.....   | 10  |
| 2.1.2 Infrared (IR) Beamline.....   | 12  |
| 2.2 Infrared Vibration Spectroscopy .....   | 14  |
| 2.2.1 Infrared Region .....   | 14  |
| 2.2.2 Vibration Spectroscopy .....  | 15  |
| Chapter Three Fourier Transform Infrared (FTIR) Microspectroscopy .....                             | 20  |
| 3.1 FTIR Spectroscopy .....   | 20  |
| 3.1.1 Generation of the Interferogram.....  | 20  |
| 3.1.2 Fourier Transformation of the Interferogram.....  | 23  |
| 3.1.3 Advantages of FTIR .....  | 25  |
| 3.2 FTIR Analysis Techniques .....  | 25  |
| 3.2.1 Transmission Method.....  | 26  |
| 3.2.2 Reflection Method.....  | 26  |
| 3.2.2.1 Specular Reflection.....  | 26  |
| 3.2.2.2 Diffuse Reflection.....   | 28  |
| 3.2.2.3 Attenuated Total Reflection (ATR).....  | 28  |

|   |    |
|---|----|
| 3.1 Infrared Microspectroscopy.....   | 30 |
| 3.2 Initial Microspectroscopical Analysis .....   | 32 |
| 3.1.1 Baseline Correction.....  | 32 |
| 3.2.2 Smoothing .....   | 34 |
| 3.2.3 Normalization.....  | 34 |
| Chapter Four Water Sampling and Analysis.....   | 37 |
| 4.1 Research Methodology.....   | 38 |
| 4.2 Water Sampling .....  | 39 |
| 4.2.1 Sampling Sites.....   | 39 |
| 4.2.2 Sampling Collection.....  | 39 |
| 4.3 Samples Analysis and Preparation .....  | 41 |
| 4.4 FTIR Analysis.....  | 43 |
| Chapter Five Chemical Characterization of the Dissolved Organic Matter                          | 45 |
| 5.1 Chemical Characterization of Dissolved Organic Matter in the Solid<br>Samples .....         | 48 |
| 5.2 Identification More Important Chemical Compounds .....                                      | 54 |
| 5.3 Discussion.....   | 58 |
| 5.3.1 Chemical Characterization of Dissolved Organic Matter in all<br>Solid Samples .....       | 58 |
| 5.3.2 Chemical Characterization of Dissolved Organic Matter from the<br>Same Point Source ..... | 59 |
| Chapter Six Conclusions and Recommendations .....   | 60 |
| 6.1 Conclusions.....  | 60 |
| 6.2 Future recommendations .....  | 61 |
| References .....  | 62 |
| المخلص .....  | ب  |

## List of Figures

|   |    |
|---|----|
| <b>Figure 1.1:</b> Map of the distribution of synchrotron radiation sources around the world .....  | 8  |
| <b>Figure 2.2:</b> Map of the SESAME location.....  | 9  |
| <b>Figure 2.3:</b> Picture of SESAME building .....   | 10 |
| <b>Figure 2.4:</b> Layout of SESAME machine.....  | 11 |
| <b>Figure 2.5:</b> The unit cell of the SESAME storage ring .....   | 12 |
| <b>Figure 2.6:</b> The schematic diagram of the IR beamline design .....  | 13 |
| <b>Figure 2.7:</b> The end station of IR beamline at SESAME is equipped the 8700 Thermo Scientific© FTIR spectrometer coupled with the Thermo Scientific© Nicolet Continuum IR-microscope.....  | 14 |
| <b>Figure 2.8:</b> Spectral regions of electromagnetic radiation, with expansion of IR region .....   | 15 |
| <b>Figure 2.9:</b> Schematic representation the stretching and bending vibrational modes .....  | 16 |
| <b>Figure 3.1:</b> Schematic of the Michelson interferometer .....  | 21 |
| <b>Figure 3.2:</b> An example of single beam of our DOM sample converted to transmission spectrum :(a) Single beam spectrum and background, (b) transmission spectrum after subtraction of the background from the single beam spectrum ..... | 24 |
| <b>Figure 3.3:</b> An example of specular reflection .....  | 27 |
| <b>Figure 3.4:</b> An example of reflectance-absorbance .....   | 27 |
| <b>Figure 3.5:</b> Diffuse reflection by a powder .....   | 28 |
| <b>Figure 3.9:</b> An absorption spectrum before and after base line correction using Rubberband correction of our DOM sample.....  | 33 |
| <b>Figure 3.10:</b> An absorption spectrum before and after auto baseline correction of our DOM sample .....  | 33 |

|  |    |
|--|----|
| <b>Figure 3.11:</b> A transmission spectrum before and after smoothing of our DOM sample .....   | 34 |
| <b>Figure 4.1:</b> Research Methodology .....  | 38 |
| <b>Figure 4.2:</b> Location map of selected sampling sites .....   | 40 |
| <b>Figure 4.3:</b> COD testing preparation: (a) preparation of vials (b) All vials are placed into reactor for two hrs (c) testing the COD concentration by colorimeter .....  | 41 |
| <b>Figure 4.4:</b> Solid samples preparation for FTIR analysis: (a) filtering all water samples using paper filter from mm to micrometer to get DOM (b) evaporation the filtered water to get suspended solid. ....  | 43 |
| <b>Figure 5.1:</b> FTIR spectra of sample (1): (a) FTIR spectra of four points in the sample, (b) average spectrum of four points .....  | 49 |
| <b>Figure 5.2:</b> FTIR spectra of sample (2): (a) FTIR spectra of four points in the sample, (b) average spectrum of four points .....  | 51 |
| <b>Figure 5.3:</b> FTIR spectra of sample (3): (a) FTIR spectra of four points in the sample, (b) average spectrum of four points .....  | 52 |
| <b>Figure 5.4:</b> FTIR spectra of all three solid samples from different points along wadi Al-Badan: sample1 from point 1, sample 2 from point 2, sample 3 from point 3 .....   | 54 |
| <b>Figure 5.5:</b> FTIR spectra (blue line) and secondary derivative (green line) of the solid samples in the range 1000-1800 $\text{cm}^{-1}$ from different points along Wadi Al-Badan: (a) Sample 1 from point1, (b) sample 2 from point 2, (c) sample 3 from point 3 ..... | 56 |

## List of Tables

|   |    |
|---|----|
| <b>Table 2.1:</b> General IR Absorption Frequencies .....   | 18 |
| <b>Table 4.1:</b> Wastewater strength in term of COD test .....   | 42 |
| <b>Table 4.1:</b> Routine analysis results for COD test .....   | 42 |
| <b>Table 5.1:</b> General assignments of FTIR spectra of DOM fractions .....  | 46 |
| <b>Table 5.2:</b> Peak assignements in FTIR spectra of all three solid samples.   | 47 |
| <b>Table 5.3:</b> Peak intensities in FTIR spectra of all three solid samples .....   | 47 |
| <b>Table 5.4:</b> Peak assignments and positions of each compound class in<br>secondary derivative FTIR spectra of all three solid samples. | 57 |

# **Characterization of Dissolved Organic Matter in Wadi Al-Badan using Fourier Transform Infrared Microspectroscopy at SESAME**

**By**

**Amal Atari**

**Supervisor**

**Dr. Ahmed Bassalat**

**Co-Supervisor**

**Dr. Sameer Shadeed**

## **Abstract**

Wadi Al-Badan is one of the Faria catchment tributaries that drains from the eastern parts of Nablus city. Water quality in the Wadi is being deteriorated due to the continuous effluent of untreated wastewater from the city of Nablus. Contamination by Dissolved Organic Matter (DOM) is a predominant problem in the Wadi which in turn can activate microorganisms growth in the Wadi flow. The presence of microbiological contaminants will potentially contaminate the surface water and groundwater resources in the catchment. The contaminated water will endanger the local consumers mainly those who use water for drinking purposes. Therefore, it is important to study and characterize the DOM in Wadi Al-Badan. Selected water samples were collected along the main Wadi (stream flow) and analyzed using two methods: firstly, traditional analysis that was conducted at the labs of the Water and Environmental Studies Institute (WESI) of An-Najah National University and secondly, using FTIR analysis at Synchrotron light for Experimental Science and Applications (SESAME) in Jordan. For FTIR analysis, after survey spectra were obtained, they were analyzed using Essential FTIR software, which allows for identifying various peaks of DOM components. FTIR results showed that the considerable presence of

different compounds of DOM are: Amide, aromatic, aliphatic, and carbohydrate compounds. In addition, DOM chemical compositions are affected by DOM inputs from the surrounding environment and natural purification that take place along the main Wadi. The study demonstrated that FTIR method could be used to characterize DOM in aquatic system, as well as to track the potential sources of DOM in Wadi flow.

# **Chapter One**

## **Introduction**

# Chapter One

## Introduction

### 1.1 General Background

Water is considered as one of the most important and sensitive issues in the Middle East in coming years. Palestine (defined as West Bank and Gaza strip) is one of the Middle East countries that sufferer from water scarcity [1]. The majority of water supply resources available to the Palestinian in West Bank come from ground water. Future population growth and its associated water demands are expected to place severe pressure on the limited ground water resources reserves. Moreover, these resources are being deteriorated to continuous discharge of untreated wastewater from Palestinian cities into receiving waters and uncontrolled agricultural practices [2].

Organic Matter is an example of contaminates present mostly in wastewater. It is defined as a complex mixture of aromatic and aliphatic hydrocarbons with functional groups such as amides, carboxyl, and hydroxyl [3]. Two kinds of the organic matter are identified, which are the suspended and dissolved fraction. The dissolved organic matter can enter to water from various resources, either natural or human activities, such as that added biosolids to the soil or through the addition of industrial and domestic wastewater and effluent from landfill to environment.

Organic Matter is traditionally characterized by different methods such as Chemical Oxygen Demand (COD) [4]. In addition to traditional methods, Fourier Transform Infrared (FTIR) spectroscopy has been used as a new analytical method since it can provide detailed information about the molecular composition materials in term of Functional groups. Fundamentally, infrared spectroscopy is based on the vibration of molecules when they are exposed to infrared radiation and each bond in the molecule has different vibration modes: stretching and bending.

This thesis focuses on the Dissolved Organic Pollutant in aquatic system because its chemical composition provides information about the water quality and the linkage of it sources.

## **1.2 Research Problem**

The raw of wastewater from eastern part of Nablus City is discharged into Wadi Al-Baden without any treatment. Wadi Al-Badan stream flow is going to pollute mixed spring fresh water along Al-wadi. The rest of it also infiltrates into ground water body and consequently pollutes water resources in the catchment [5]. Domestic and industrial wastewater is containing large number of pollutants, which are considered as bio-toxic pollutants and are subject to degradation by natural purification. Pollutions like organic matter have negative health impact and may cause contamination to drinkable water by activating the growth of microorganism in water system [6]. Therefore, it is very important to characterize them in water and this will help planners in

their decision making and management planning for catchment pollutant level.

### **1.3 Research Objective**

The main goal of this research is to assess the presence of Dissolved Organic compounds in Wadi Al-Badan stream flow. In light of the above, the following objectives are achieved:

1. To develop water sample preparation procedure for characterization of Dissolve Organic Matter (DOM) using Fourier Transform Infrared (FTIR) microspectroscopy analysis.
2. To investigate the use of the sample preparation and FTIR analysis for characterizing the DOM in water from several locations in Wadi-Al-Badan.
3. To assess water natural purification of DOM along Wadi Al-Badan.

### **1.4 Thesis Outline**

The thesis is arranged in six chapters. Chapter one presents the general background, research objectives, and research problem. Chapter two provides information about synchrotron light and its application and shows the synchrotron facility in Middle East (SESAME): its storage ring and IR beamline. It also provides information about IR vibration spectroscopy technique. Chapter three presents FTIR work and its advantages. It then provides information about infrared sampling technique and the initial microspectroscopical analysis. Chapter four presents the overall of the

research methodology including water sampling, sample analysis, and FTIR analysis. Chapter Five presents the major chemical compounds of DOM in all samples. Chapter six presents the conclusions and the recommendations for the future work.

**Chapter Two**  
**Application of Synchrotron**  
**Radiation**

## **Chapter Two**

### **Application of Synchrotron Radiation**

Synchrotron radiation is generated when charged particles moving at speed close to the speed of light are forced to move along curved trajectories by applied magnetic fields. It got its name after it was discovered in an electron synchrotron of the General Electric Company (USA) in 1947 [7]. Synchrotron radiation spans from far infrared to hard x-rays. It is characterized by high brightness which is defined as number of photons, per unit sources size and divergence in a given bandwidth, and high collimation and highly degree of polarization.

Due to the special properties of synchrotron radiation, most of accelerators today are not dedicated to accelerator physics but exist to generate synchrotron radiation for scientific experiments. Synchrotron radiation is used in many applications such as physics, chemistry, material science, and environmental science. One of the fast growing applications of synchrotron radiation is in environmental biochemistry research [8]. For example, by combining synchrotron light and analytical techniques, it has been possible to study element distribution in various environmental samples such as atmospheric dust, plants, soils, and sediments and various waste materials, etc. In this thesis, Fourier Transform Infrared (FTIR) microspectroscopy was used as a new analytical technique to study the dissolved organic contaminates in water.

The worldwide distribution of synchrotron facilities shows that they are spread across all continents as shown in Figure 1.1. SESAME is the only synchrotron facility in the Middle East and it is the place where this work has been performed, and it will be presented in the next section.



**Figure 1.1:** Map of the distribution of synchrotron radiation sources around the world.

## 2.1 Synchrotron-light for Experimental Science and Applications in the Middle East (SESAME)

SESAME is the only synchrotron facility in the Middle East located in Allan-Jordan, as shown in Fig 2.2. It is a collaborative project by scientists and government of the region set up as the model of CERN (European Organization for Nuclear Research) although it has very different scientific aims. The project aims at promoting science and technology in the Middle East, as well as promoting international relation. Figure 2.3 shows the overview of SESAME building.

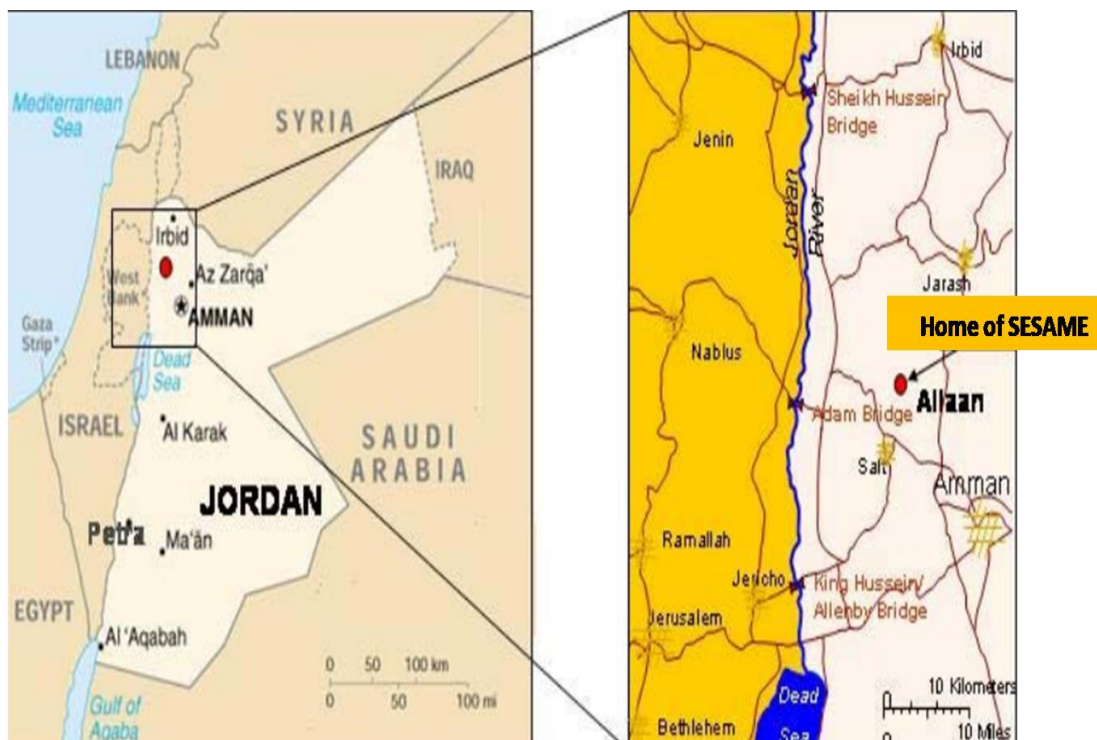


Figure 2.2: Map of the SESAME location [9].



**Figure 2.3:** Picture of SESAME building.

### **2.1.1 Storage Ring**

The SESAME layout, as shown in figure 2.4, consists of three main parts: the microtron, the booster ring, and the storage ring [10]. The electrons are injected from a 20 MeV microtron into an 800 MeV booster synchrotron. The 800 MeV beam is transported through the transfer line to the main storage ring where the energy of the electron is ramped up to 2.5 GeV and the electron beam is forced to follow curved trajectory by dipole magnet. At each dipole, the electron beam is deflected and synchrotron radiation is emitted and extracted through beamline.

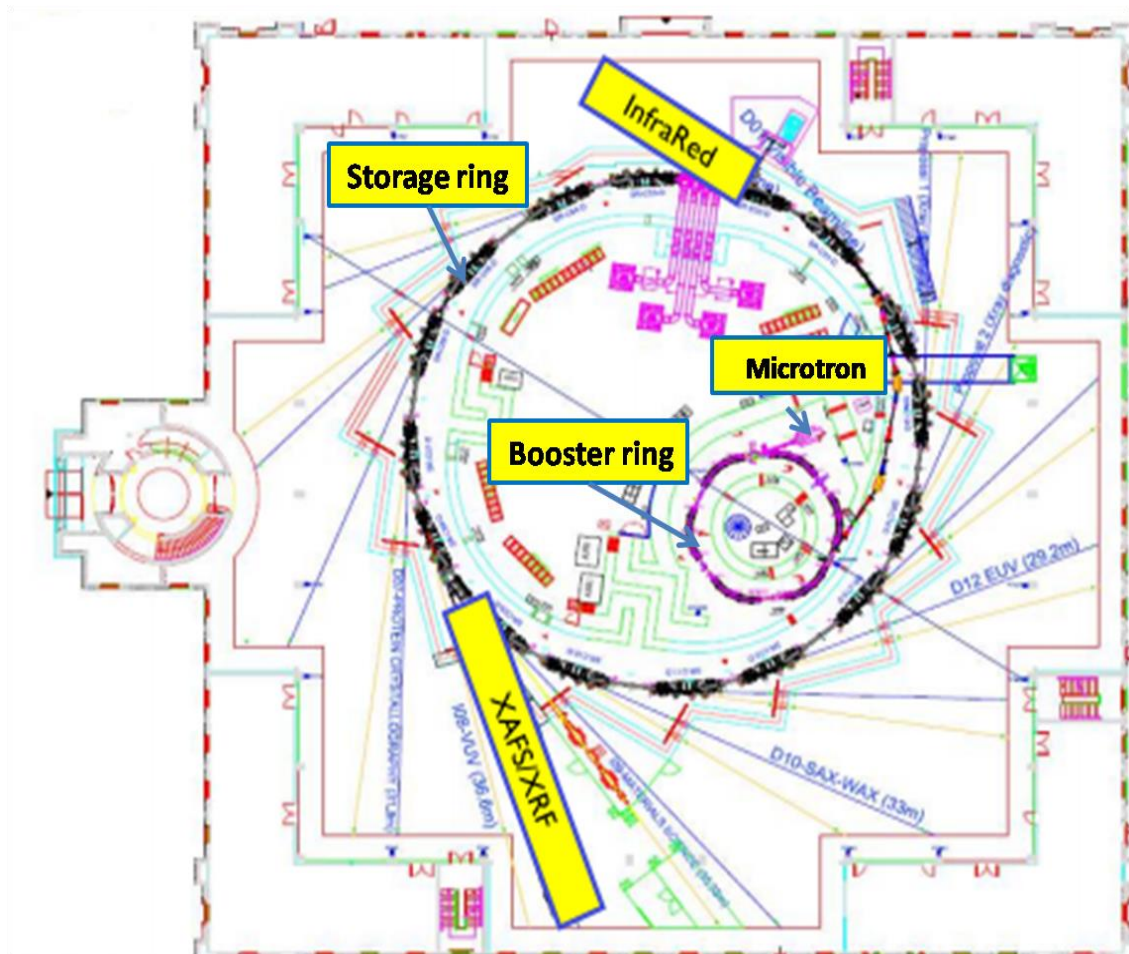


**Figure 2.4:** Layout of SESAME machine [11].

The storage ring, with overall length of 133.2 m, consists of 8 cells, each cell holds two dipoles (usually called bending magnet) and a straight section between them. The unit cell of SESAME storage ring is shown in figure 2.5, which consists of arrangement of magnet with 16 in total. Each unit cell has two bending magnet, six quadrupoles for particle beam focusing and eight sextupoles to control the chromatic and geometric aberrations.

As for beamline around the storage ring, it consists of many specially-designed optical components which are dedicated to transport synchrotron radiation from the bending magnets into users' experimental end

stations. There are two beamlines in operation at SEAME: IR and XAFS/XRF beamlines.

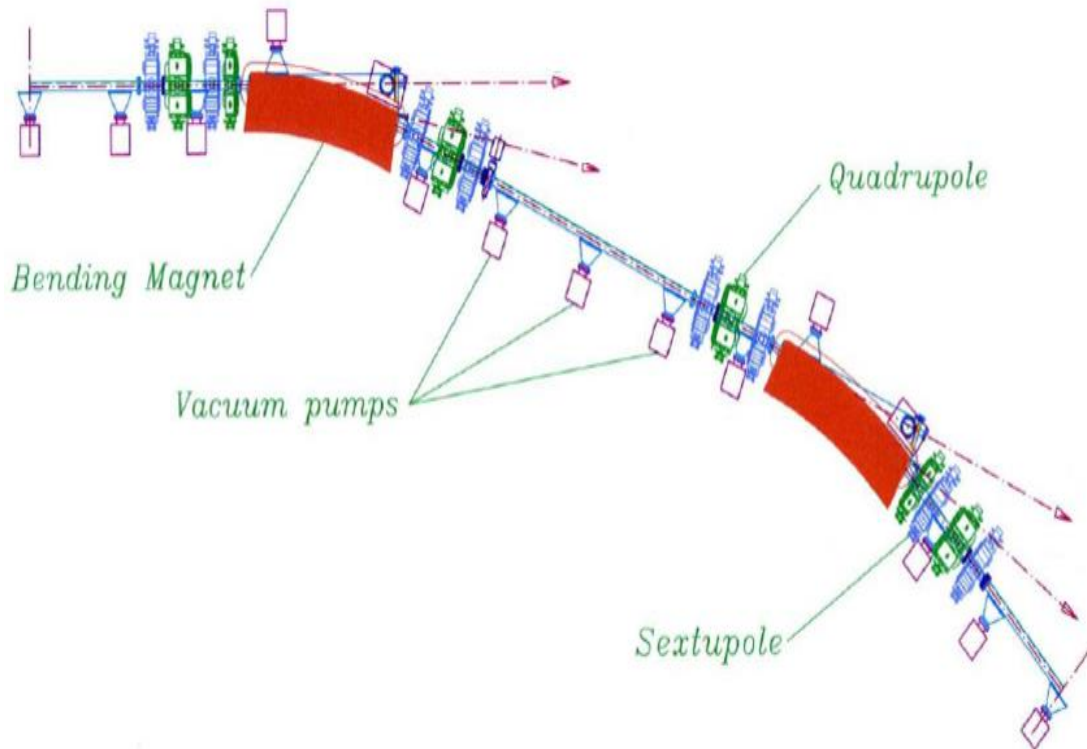


**Figure 2.5:** The unit cell of the SESAME storage ring [12].

### 2.1.2 Infrared (IR) Beamline

The IR beamline is the second completely new beamline at SESAME that has been successfully designed to transfer synchrotron infrared radiation from a bending magnet of the storage ring SESAME to the experimental end station. It is conducted in various application fields ranging from surface science, Biomedical Diagnostics, Environmental Science, Surface and Material Science, Archaeology, Cultural Heritage, Art restoration, Geology, and many others [13].

The Synchrotron IR beamline consists of two critical components: the extraction chamber located inside the tunnel wall that consists of two flats and one focusing mirror. The second one is the beam splitting system, located in the experimental floor to optimize coupling of the synchrotron IR beam with the FTIR spectroscopy. Figure 2.6 shows schematic diagram of the top view of IR beamline at SESAME. The infrared beam is extracted horizontally and is then focused to a CVD diamond exit window outside the tunnel wall. After that, the beam is focused right inside the radiation shield wall then the beam is diverted right into the spectrometer system.

The end station of IR contains IR microscope and FTIR interferometer as shown in figure 2.7. The coupling box located before spectrometer is used to reshape the beam and monitor its position at the interferometer input.

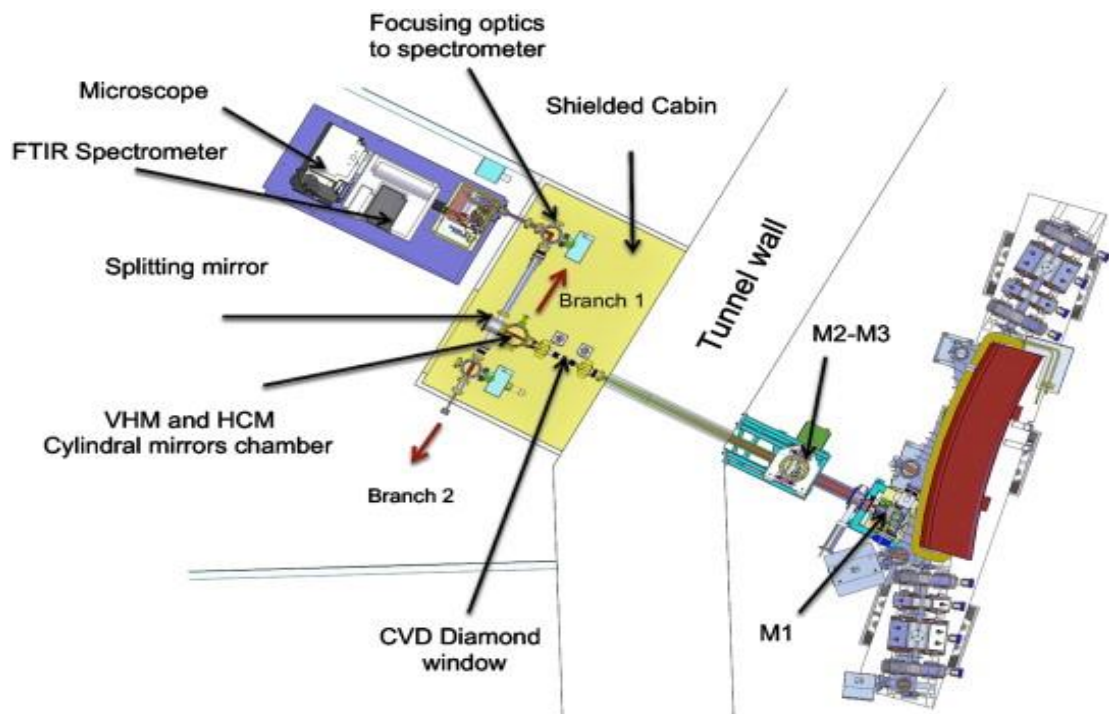


**Figure 2.6:** The schematic diagram of the IR beamline design.



**Figure 2.7:** The end station of IR beamline at SESAME is equipped the 8700 Thermo Scientific© FTIR spectrometer coupled with the Thermo Scientific© Nicolet Continuum IR-microscope.

## 2.2 Infrared Vibration Spectroscopy

### 2.2.1 Infrared Region

Electromagnetic spectrum is classified into different regions according to wavelength and wave number ( $k$ ) where  $k = \frac{1}{\lambda(\text{cm})}$ . The main regions of the electromagnetic spectrum are radio waves, microwaves, infrared radiation, visible light, ultraviolet radiation, X-rays and gamma rays, as shown in Figure 2.8.

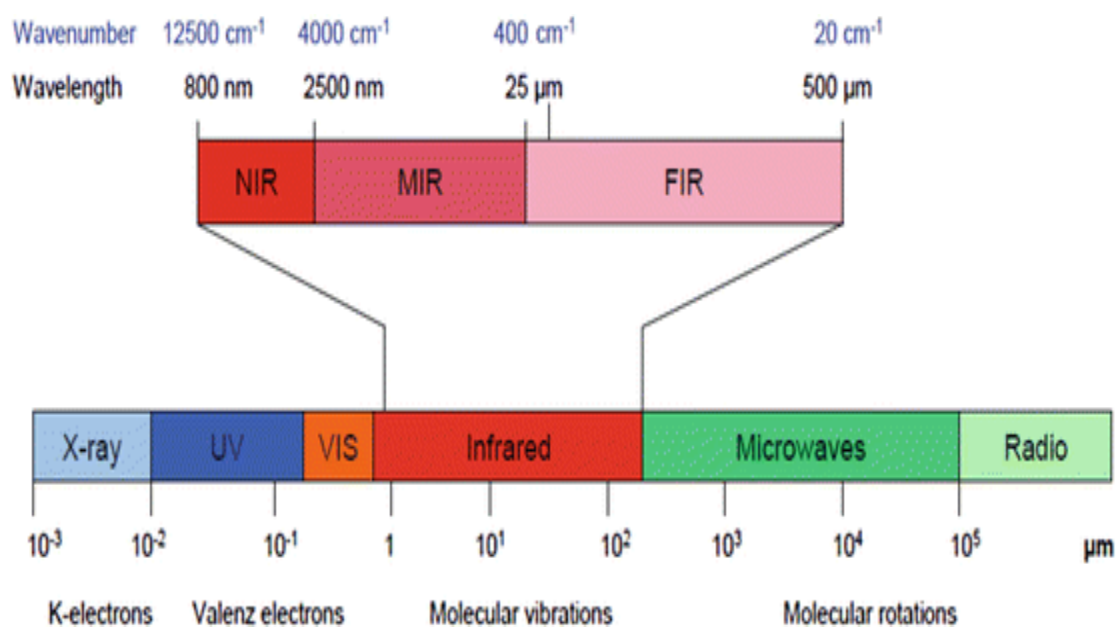


**Figure 2.8:** Spectral regions of electromagnetic radiation, with expansion of IR region [14].

As shown in Figure 2.8, the IR spectral region of the electromagnetic spectrum extends from the microwave to visible region. It includes radiation with wave number ranging from (14000 to  $20 \text{ cm}^{-1}$ ) and is divided into three regions: Far-Infrared ( $400\text{-}20 \text{ cm}^{-1}$ ), mid-Infrared ( $4000\text{-}400\text{cm}^{-1}$ ), and near Infrared ( $12820\text{-}4000 \text{ cm}^{-1}$ ).

### 2.2.2 Vibration Spectroscopy

Light can interact with matter in different ways, absorption, transmission, and reflection. The chemical bonds vibrate when the matter absorbs IR radiation. Thus, the existence of chemical bonds is a necessary condition for infrared absorbance. Molecule absorbs infrared radiation, when the vibrations of these bonds result in change of the molecule's dipole moment [15].

Each molecule has constant motions: translation, rotation, and vibration motions. For molecule with N number of atoms, it has  $3N$  degrees of

freedom, six motions are for translations and rotations of the molecule. This leaves  $3N-6$  degrees of vibration freedom for nonlinear molecules and  $3N-5$  for linear molecule, because rotation about its molecular axis cannot be observed. Vibrations can involve two types: stretching or bending. Stretching is a symmetrical and asymmetrical stretching movement of bond axes. The bending vibration occurs when the bond angle is changed. These motions are known as scissoring, wagging, rocking, and twisting. Figure 2.9 shows the stretching and bending modes.

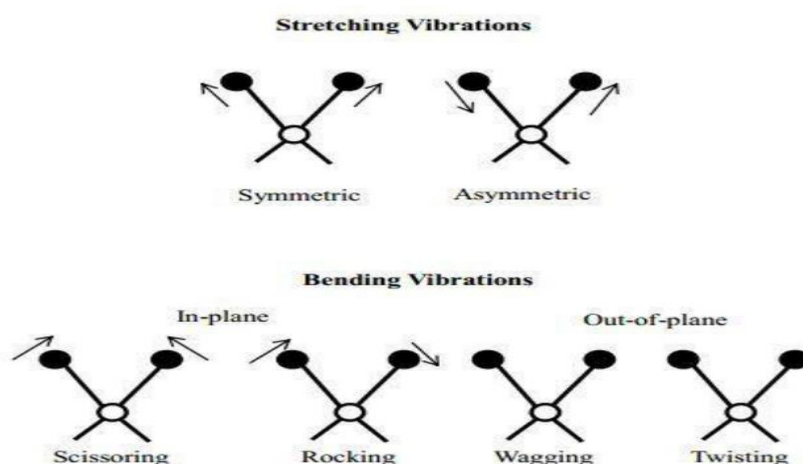


**Figure 2.9:** Schematic representation the stretching and bending vibrational modes [16].

The absorbed frequency depends on several factors: type of vibration, strength of bonds, and masses of atoms at each bond. Generally, it is easier to bend than to stretch, so frequency absorptions due to bending occur at lower wavenumbers than stretches for the same bond. The strength of the bond can be characterized by proportionality constant termed the force constant ( $K$ ) and the reduced mass ( $\mu$ ) expressed in terms of atomic mass as follows:

$$\mu = \frac{m_1 m_2}{m_1 + m_2} \quad (2.1)$$

Where:  $m_1$  and  $m_2$  are the masses of atoms at the end of each bond.

The equation relating the force constant, the reduced mass and the frequency of absorption ( $\gamma$ ) is derived from the model of the harmonic oscillator.

$$\gamma = \frac{1}{2\pi c} \sqrt{\frac{K}{\mu}} \quad (2.2)$$

Where

$\gamma$  = Frequency in Hertz

$c$  = Speed of light ( $3 \times 10^8$  m/s)

Infrared (IR) Spectroscopy studies the interaction of infrared light with matter, which can be used to identify unknown materials by detecting vibration that characterize the molecular bond in materials. It is commonly used to show the presence or absence of functional groups, known as specific groups of atoms or bonds within molecules that are responsible for the characteristic chemical reactions of those molecules. IR spectra can provide chemical structures as well as the concentration of a molecule in a sample from infrared spectra. Table 2.1 shows some functional groups and their frequency (wavenumber) range.

**Table 2.1: General IR Absorption Frequencies**

| <b>Bonds</b> | <b>Frequency(<math>\text{cm}^{-1}</math>)</b> | <b>Compound classes</b>                         |
|--------------|---|---|
| O-H          | 3000-2500, stretch                            | Carboxylic acid                                 |
|              | 3600-3200, stretch                            | Alcohols, Phenols                               |
| N-H          | 3300-3500, stretch                            | Amines  |
| C-H          | 2960-2850, stretch                            | Alkanes   |
|              | 1470-1350, bend                               |   |
| C-H          | 3010-3100, stretch                            | Alkenes   |
|              | 1000-675, stretch                             |   |
| C-H          | 3300, stretch                                 | Alkynes   |
| C=O          | 1670-1820, stretch                            | Aldehydes, Ketones,<br>Carboxylic acids, Esters |
| C=C          | 1600 and 1500, stretch                        | Aromatic  |
| C=C          | 1680-1640, stretch                            | Alkenes   |
| C=C          | 2260-2100, stretch                            | Alkynes   |
| C-O          | 1260-1000, stretch                            | Alcohols, Ethers, Carboxylic<br>acids, Esters   |
| C-N          | 1360-1080, stretch                            | Amines  |
| C $\equiv$ N | 2210-2260                                     | Nitriles  |
| N-O          | 1515-1560, stretch                            | Nitro Compounds                                 |
|              | 1345-1385, stretch                            |   |

**Chapter Three**  
**Fourier Transform Infrared (FTIR)**  
**Microspectroscopy**

## **Chapter Three**

### **Fourier Transform Infrared (FTIR) Microspectroscopy**

FTIR microspectroscopy is a technique that combines the infrared (IR) microscopy and the FTIR spectroscopy. The IR microscopy is used to magnify the structural details in samples, while FTIR spectroscopy provides information about molecular chemistry [17]. Together, chemical analysis can be performed with microscopic detail.

In the present study, the FTIR microspectroscopy is used to characterize dissolved organic compounds in water.

#### **3.1 FTIR Spectroscopy**

FTIR spectroscopy is one of the most common techniques used to obtain IR spectra [15]. The term FTIR spectroscopy derived from the Fourier transform (a mathematical process) which is used to convert raw data into FTIR spectrum.

##### **3.1.1 Generation of the Interferogram**

The basic components of an FTIR spectrometer are Infrared source, Michelson interferometer, and Detector, such as mercury cadmium telluride (MCT). Michelson interferometer is the main part of FTIR spectrometer which is shown in Figure 3.1. It consists of a beam splitter, fixed and removable mirrors which are placed perpendicular to the axis.

The beam splitter divides the incoming beam into two beams with equal Amplitudes by reflection and transmission. One beam travels toward the fixed mirror where it is reflected back and the other beam travels toward movable mirror where it is reflected, so the two beams travel different paths. After being reflected back, the two light beams interfere at the beam splitter which is then detected by the detector. The intensity of these two beams in the detector is measured as a function of the difference of their paths. This signal is called interferogram [18].

A scan is generated when the mirror moves once to and from. Thus, a complete interferogram is generated.

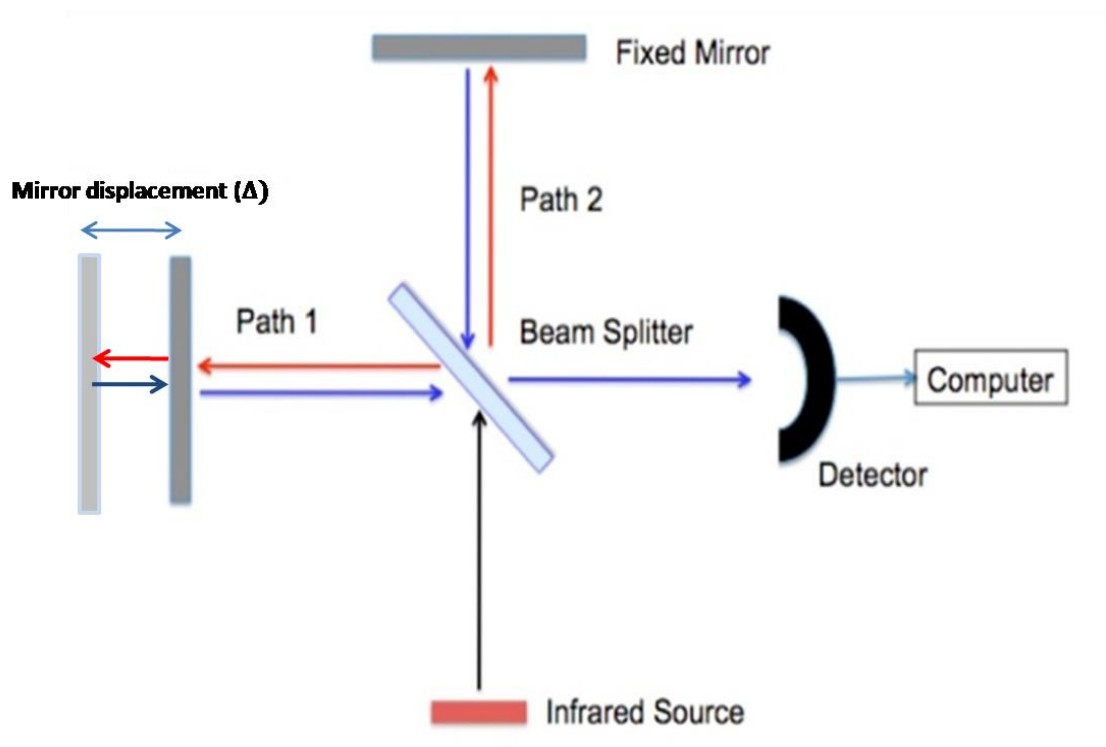


**Figure 3.1:** Schematic of the Michelson interferometer.

If the two light beams in the interferometer travel different distance, the optical path difference ( $\delta$ ), is the difference in optical distance traveled by these two beams. Zero optical path difference occurs when the two light beams travel the same distance.

Light reflected by the moving mirror travels more than the light reflected by the fixed one. The mirror displacement is the distance that the mirror is moved in interferometer and is denoted by  $\Delta$ . The relationship between mirror displacement and optical path difference is

$$\delta = 2\Delta \quad (3.1)$$

When using IR light source of wavelength  $\lambda$ , the recombinants beams, reflects off the fixed and moving mirrors, at the beamsplitter, then will be in phase. If the result is more intense than either of two beam (constructive interference), while if the result is less intense than other of two beams (destructive interference).

The constructive interference happens when

$$\delta = n \lambda \quad (3.2)$$

Where n is any integer with the values  $n = 0, 1, 2, 3, \dots$

Also the destructive interference happens when

$$\delta = \left(n + \frac{1}{2}\right) \lambda \quad (3.3)$$

Where n is any integer with the values  $n = 0, 1, 2, 3, \dots$

### 3.1.2 Fourier Transformation of the Interferogram

A spectrum is calculated by Fourier transformation (FT) of the interferogram, that is a mathematical technique used to convert the signal from time domain to frequency domain where  $I(\delta)$  is a signal of different optical path deference and  $B(k)$  is a signal of wave number as shown in equation 3.4.

$$B(k) = \int_{-\infty}^{\infty} I(\delta) \cos(2\pi k\delta) d\delta \quad (3.4)$$

After the interferogram is being Fourier transformed, sample single beam spectrum is obtained with the background spectrum. The background spectrum is subtracted from the single beam to obtain the transmission spectrum. Figure 3.2 shows an example of our single beam spectrum converted to transmission spectrum.

The transmittance spectrum (T) can be calculated as:

$$T = \frac{I}{I_0} \quad (3.5)$$

Where

T = transmittance spectrum

$I_0$  = Intensity in the background

I = Intensity in the sample spectrum

The absorbance spectrum (A) can be calculated from the transmittance spectrum using the following equation:

$$A = -\log \frac{I}{I_0} = -\log T \quad (3.6)$$

Where

A = Absorbance spectrum

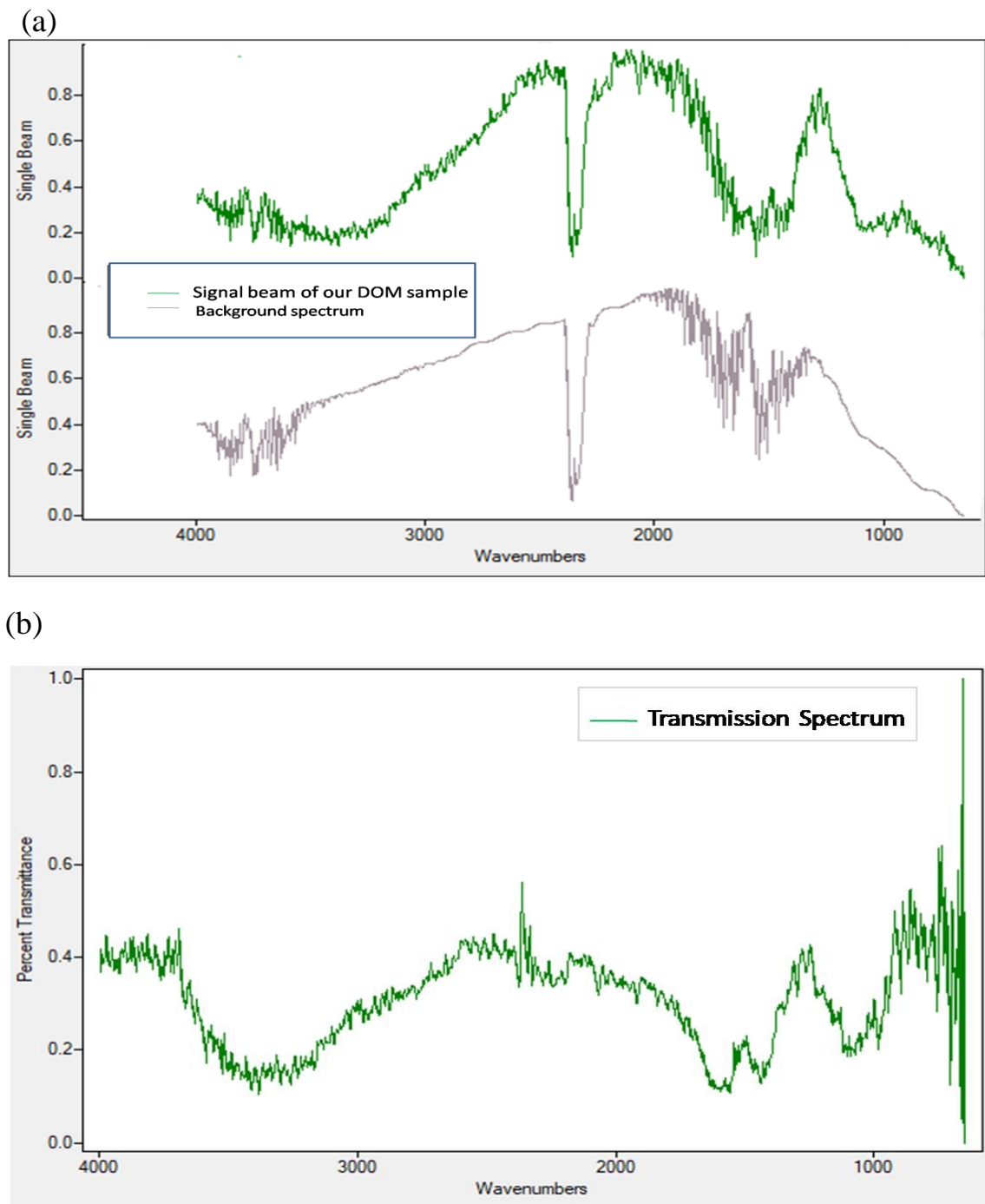


**Figure 3.2:** An example of single beam of our DOM sample converted to transmission spectrum : (a) Single beam spectrum and background, (b) transmission spectrum after subtraction of the background from the single beam spectrum.

### 3.1.3 Advantages of FTIR

FTIR spectroscopy has many advantages over dispersive IR spectroscopy, which make FTIR spectroscopy now a standard tool. One of the major advantages of FTIR spectroscopy is the rapidity in performing measurements since all source wavelengths are measured in few seconds instead of several minutes. In addition, one can collect many scans of IR spectra from the sample, which improves signal to noise ratio (SNR) because SNR is proportional to the square root of the number of scans as given by equation (3.7).

$$\text{SNR} \propto N^{\frac{1}{2}} \quad (3.7)$$

Where

SNR = Signal-to-noise ratio

N= number of scan

Another advantages are the use of few mirrors, which mean less reflective loose occurs, resulting in more energy reaching the sample and increasing the sensitivity for small IR absorption. Consequently, details in a sample spectrum will be clear. Also samples can be tested in different form such as liquid, gas, powder, solid, and film. However, FTIR spectroscopy can't detect atoms or monoatomic ions because single atoms don't contain chemical bonds.

### 3.2 FTIR Analysis Techniques

The most common analysis techniques to collect the spectral information are: the transmission and the reflection methods, we choose the method depending on the type, form, and amount of samples.

### **3.2.1 Transmission Method**

Transmission technique is the most popular technique in which the radiation passes directly through the sample. There are many advantages of this technique. It has a high SNR. It is used for analyzing different samples such as polymers, biological tissues, and organic materials. The tools that are used to prepare the samples are not expensive. The sample thickness needed for transmission measurements should be 5-30  $\mu\text{m}$  [17].

### **3.2.2 Reflection Method**

Reflection is used for samples that are difficult to analyze by the transmission method. There are many advantages of this technique.

For example, there is no thickness problem, so we can save time in preparing the sample. However, it requires special expensive accessories.

There are many types of reflection techniques, specular reflection, Diffuse Reflection, Attenuated Total Reflectance (ATR). Our FTIR measurements have been performed in Diffuse Reflection mode.

#### **3.2.2.1 Specular Reflection**

Specular reflection technique occurs when the reflection angle ( $\theta_r$ ) equals the angle of incident radiation ( $\theta_i$ ) and it used for samples that are smooth surface as shown in Figure 3.3.

If there is a coating thin film on a reflective surface, a technique called reflectance-absorbance, as shown in Figure 3.4. In this technique, one fraction of the IR light is reflected from the interface and other part

penetrates through the sample. The penetrated light is then reflected from the reflective substrate and passes again through the sample. Since the beam passes through the sample twice, the result is a “double-absorption” spectrum.

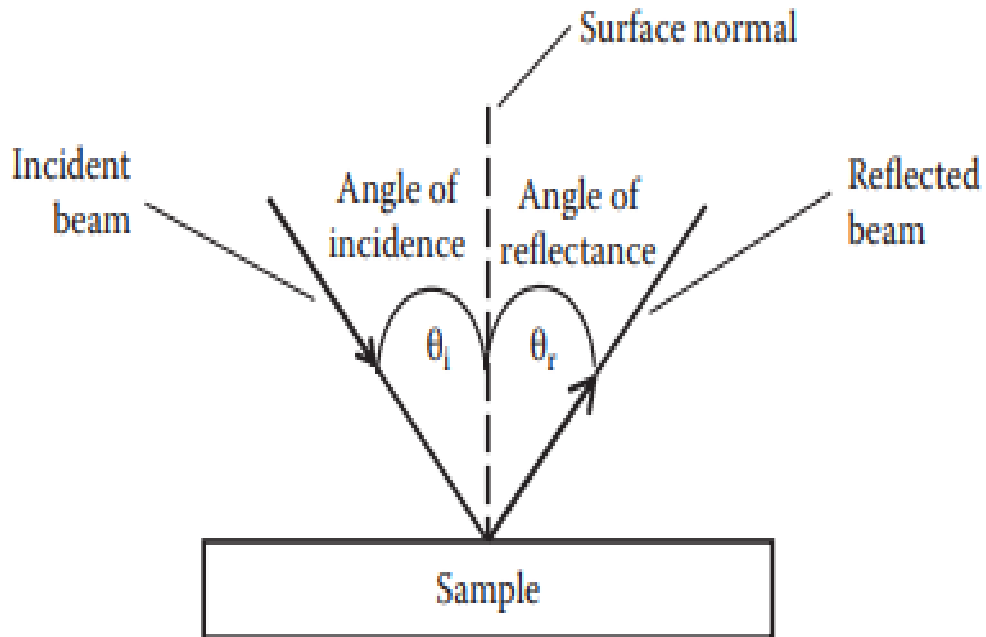


**Figure 3.3:** An example of specular reflection [18].

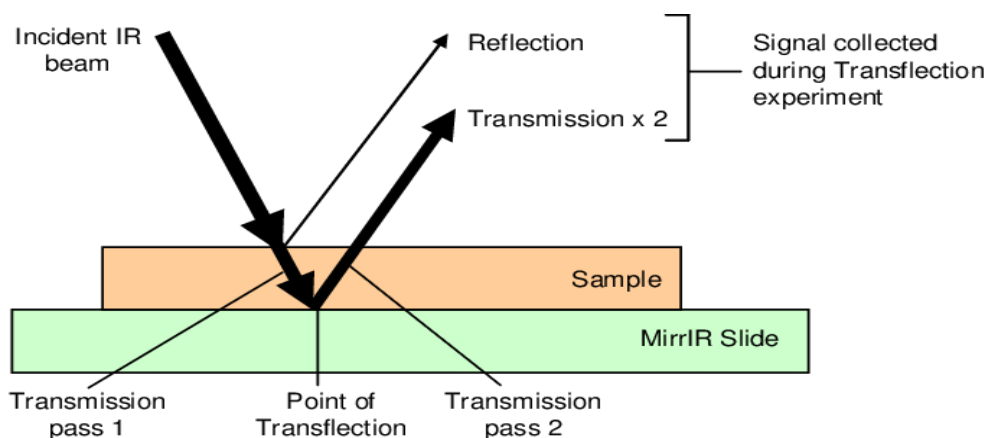


**Figure 3.4:** An example of reflectance-absorbance [19].

### 3.2.2.2 Diffuse Reflection

Diffuse reflection technique occurs for rough surface where the light penetrates through the sample is reflected in all direction. This technique is used for powder and fiber sample. To prepare powder sample, it mixed with KBr powder to reduce particle size and avoid light scattering.

Figure 3.5 shows a schematic of diffuse reflection from powder sample.

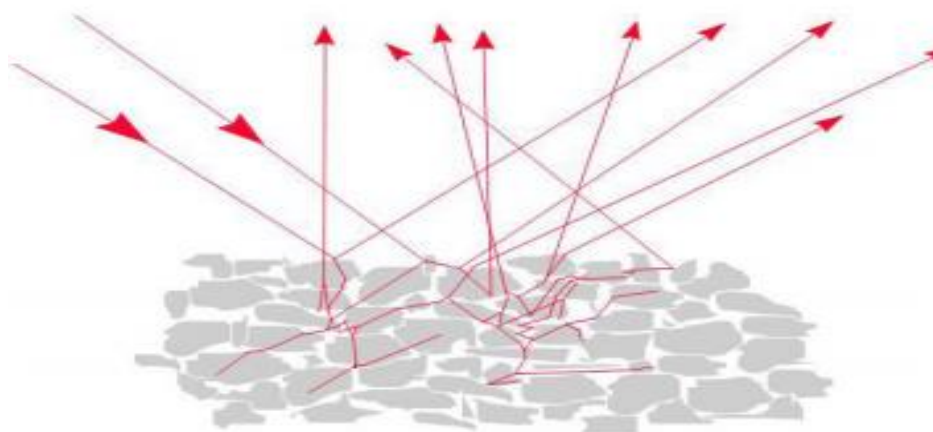


**Figure 3.5:** Diffuse reflection by a powder [20].

### 3.2.2.3 Attenuated Total Reflection (ATR)

Attenuated total reflection (ATR) is based on the concept of total internal reflection [18]. An internal reflection occurs when IR beam light traveling through a crystal of high refractive index ( $n_c$ ) is incident into sample with lower refractive index ( $n_s$ ). The IR beam entering the crystal is totally internally reflected within the crystal. The beam creates an evanescent wave that penetrates into the sample as shown in Figure 3.6 Some of the energy of evanescent wave then will be absorbed by the sample and its intensity is reduced (attenuated) in regions of the ATR spectrum.

Attenuated total reflection technique used in material that are thick and cannot be cut into thin sections or strongly absorbing IR light such as liquids, rubber and plastic.

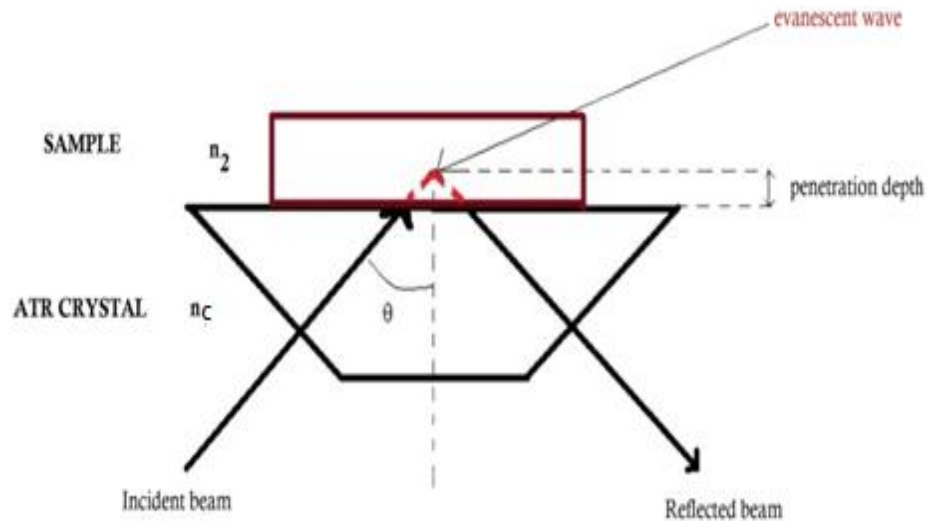


**Figure 3.6:** Graphical representation of the evanescent waves that penetrate into the sample [21].

The depth of penetrate (DP) is defined as depth at which the evanescent wave intensity decreases to  $(\frac{1}{e})$  of its value at the surface which given in equation:

$$DP = \frac{1}{2kn_c(\sin^2\theta - n_{sc}^2)^2} \quad (3.8)$$

Where:

$k$  = wave number

$n_c$  = Refractive index of ATR crystal

$\theta$  = Angle of incident beam

$$n_{sc} = \frac{n_{\text{sample}}}{n_{\text{crystal}}}$$

### 3.1 Infrared Microspectroscopy

Coupling of the microscope to an infrared spectrometer is defined as microspectroscopy. In this research, we use a special type of microscope known as (IR microscope).

The IR microscope works in two modes: visible and infrared. Figure 3.7 shows schematic diagram of IR microscope.

Infrared microscopes are similar to conventional microscopes, with the exception that the optics are mirrors instead of lenses, allowing the IR beam to pass through the instrument with minimum IR absorption [22].

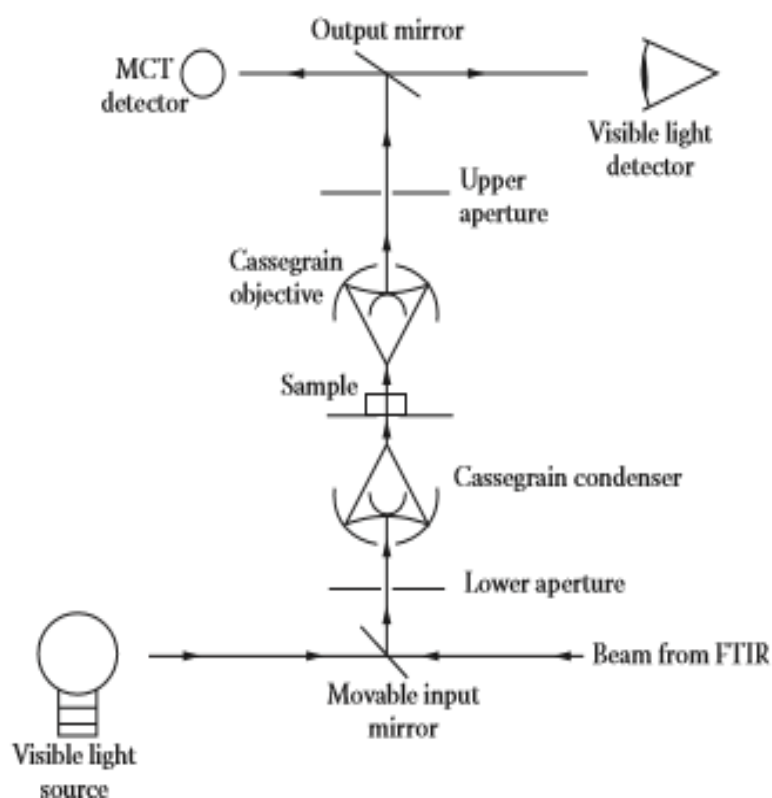


**Figure 3.7:** Optical diagram of IR microscopy used for FTIR microscopy [18].

IR microscopes have two modes of data collection: transmission and reflection modes. Figure 3.8 shows the transmission and reflection modes in IR microscope.

In transmission mode, the IR light is focused into the sample through illuminating objective. The IR light then is transmitted through the sample and collected by collecting objective. The output light is then transferred to a detector.

In reflection mode, the IR light that comes from above is focused into the sample and is collected after reflection from the sample by the upper collecting objective since the upper collecting objective acts as both illuminating and collecting objective, so the lower half of the microscope is not used.

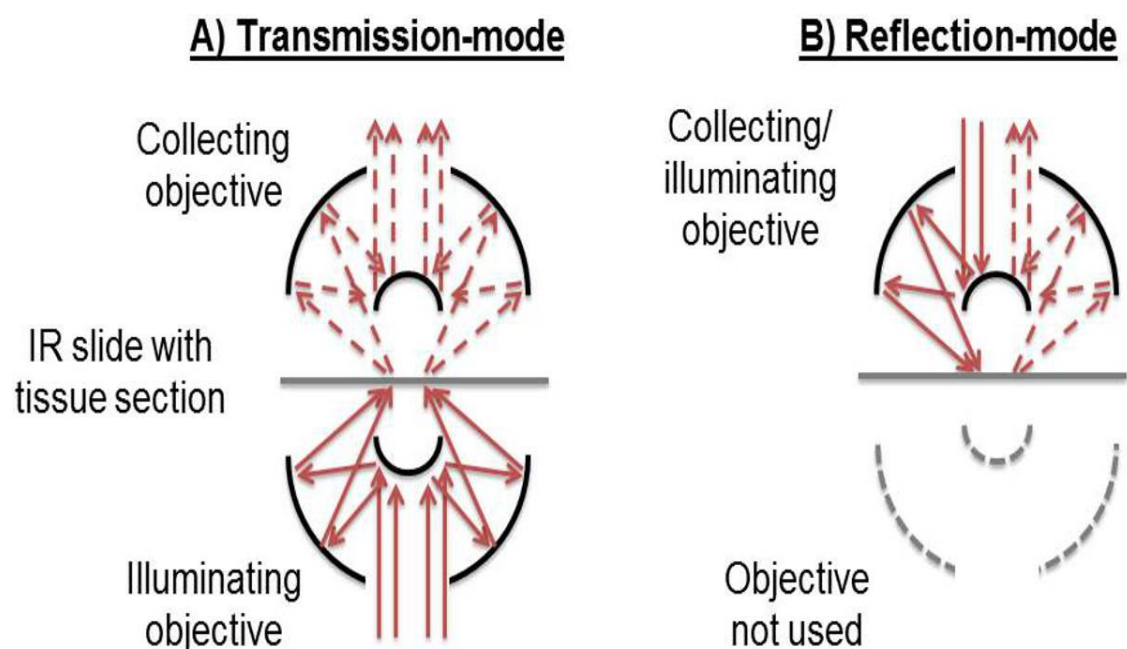


**Figure 3.8:** Optic diagram of IR microscope in two modes: (A) transmission mode (B) reflection mode [23].

## **3.2 Initial Microspectroscopical Analysis**

Essential FTIR software allows for performing various spectral analysis steps for Infrared spectrum as shown in the next section:

### **3.1.1 Baseline Correction**

There are many reasons that make the spectral baseline not flat like sample scattering, inappropriate choice of background and instrument drift [18]. In these cases, the spectral processing technique can be used to correct curved baseline of spectra called baseline correction. Figure 3.9 shows an example of an absorption spectrum before and after baseline correction using “Rubberband” correction. The baseline correction is generated as follow: First, we generate curve that is closely parallels to the spectrum baseline. Secondly, we subtract this curve from the spectrum, yielding a spectrum without a baseline.

In essential FTIR software, it provides the Rubberband correction method to correct the spectrum baseline. In rubberband correction method, the given spectrum is dived to N ranges, and then initial baseline is built by picking the lowest point in the spectrum. After that, the baselines are piecewise linear through the support points.

In essential FTIR software, it provides also auto baseline correction tool to repair simple baseline defects without defining Regions, which has been used in this work. An example of the Auto Baseline Correction is shown in Figure 3.10.

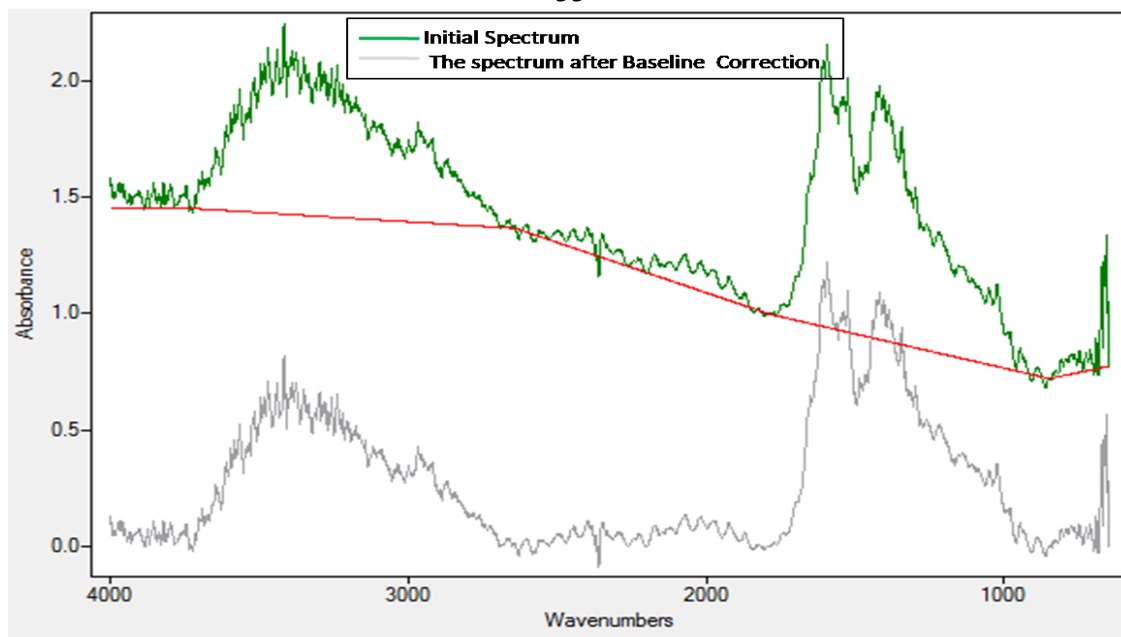


**Figure 3.9:** An absorption spectrum before and after base line correction using Rubberband correction of our DOM sample.

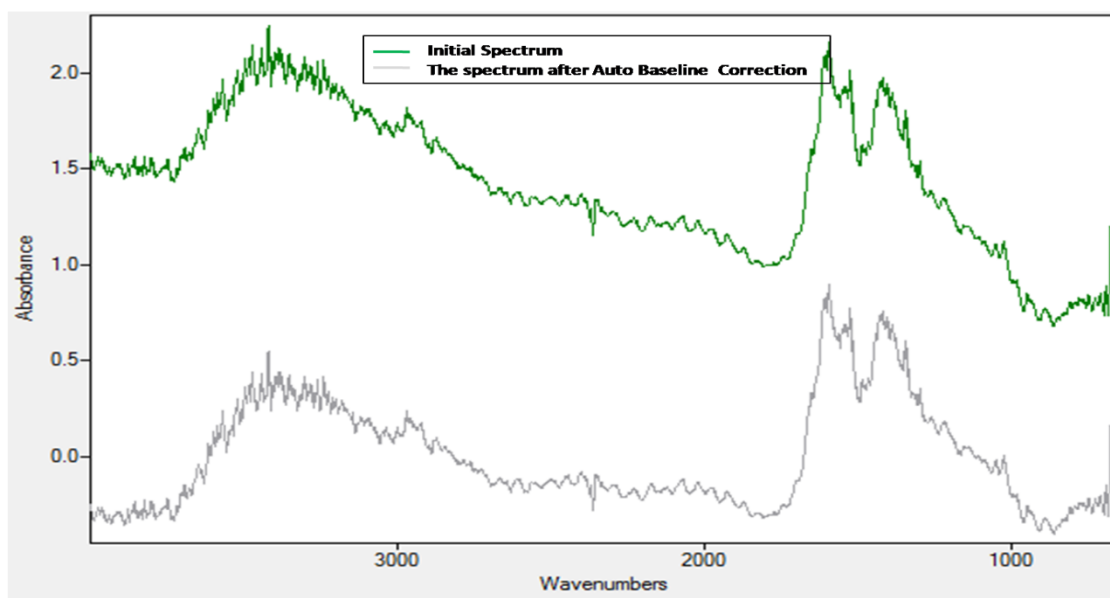


**Figure 3.10:** An absorption spectrum before and after auto baseline correction of our DOM sample.

### 3.2.2 Smoothing

Smoothing is used on noisy spectra to reduce the noise level, so features that may have been hidden under the noise can be seen well [15].

It works by calculating the average transmission or absorption spectrum as group of data points called smoothing window and the size of smoothing window is determining the number of data point to use in average spectrum. An example of smoothing spectrum of our DOM spectrum using 45 smoothing window is shown in Figure 3.11.

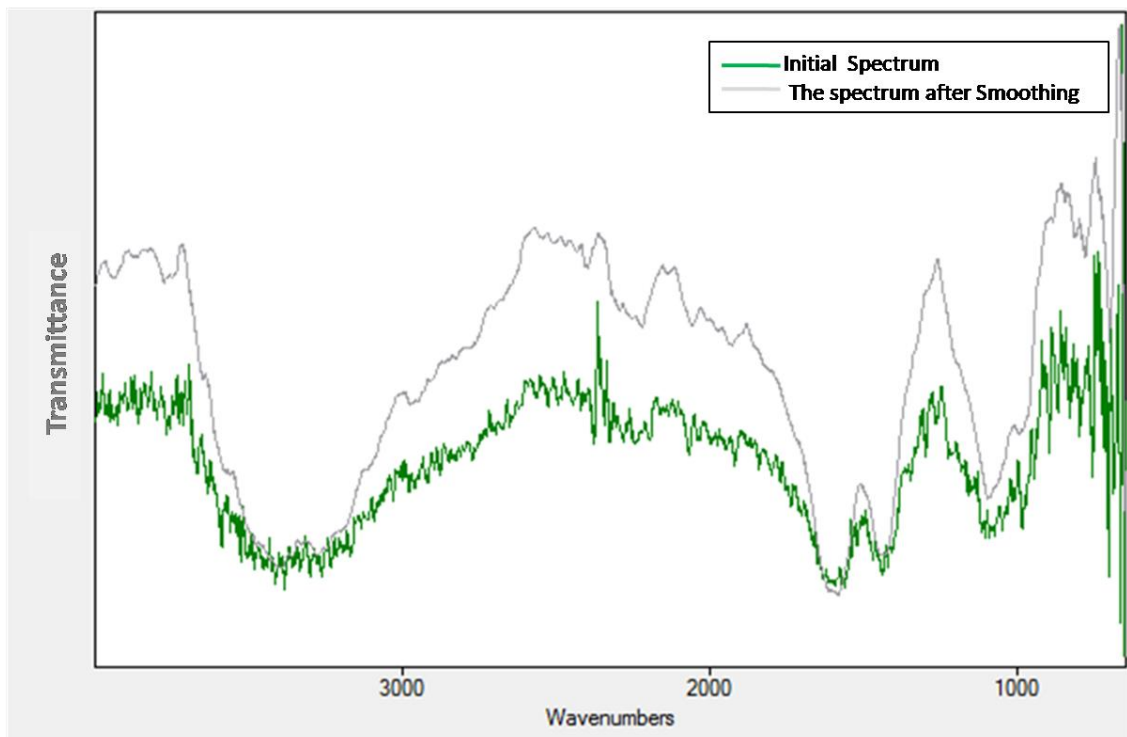


**Figure 3.11:** A transmission spectrum before and after smoothing of our DOM sample.

### 3.2.3 Normalization

Normalization is a tool used for comparing spectra from different samples. One type of normalization is known as Min-Max Normalization, which is used to normalize our spectra. The min-max normalization shifts the spectra

so the minimum y-value is set to zero and the maximum y-value is expanded to 1 absorbance unit, so that we easily compare the samples and conditions.

## **Chapter Four**

# **Water Sampling and Analysis**

## Chapter Four

### Water Sampling and Analysis

The main objective of the research is the characterization of the water pollutant content in Palestine using FTIR Microspectroscopy. First water samples have been collected in November 2017 from the main spring and wells that feed Nablus city in Palestine. Water samples have been then analyzed by the 8700 Thermo Scientific© FTIR spectrometer equipped with the Specac's Omni Cell liquid transmission accessory. This accessory is used to control the water pathlength in different size as 1mm, 0.05mm, and 0.025mm spacer.

Water is the dominating infrared absorber in aqueous solutions and the small concentrations of pollutants give weak signals that are covered by the water absorbance spectrum. To measure the small concentration of pollutants require exposing of large unwanted absorption spectrum caused by water to obtain small needed spectrum of pollutants. The procedure involves reducing of water absorption spectrum by using different pathlengths and then subtracting it from water sample spectrum to get the pollutants. The problem we faced in performing this procedure is that the FTIR results are just water and no any difference could be sensed, even when the smallest pathlengths of water are used. The solution to solve this problem is trying to find new method to expose of water technically and search for certain type of pollutants which can be detected by FTIR. To achieve the above objective, the road of map is modified as shown in next section.

## 4.1 Research Methodology

Due the lessons learned from first method, the road map of the research is used to achieve the aim of the research. Figure 4.1 below gives a complete overview of the steps followed in carrying out this research.

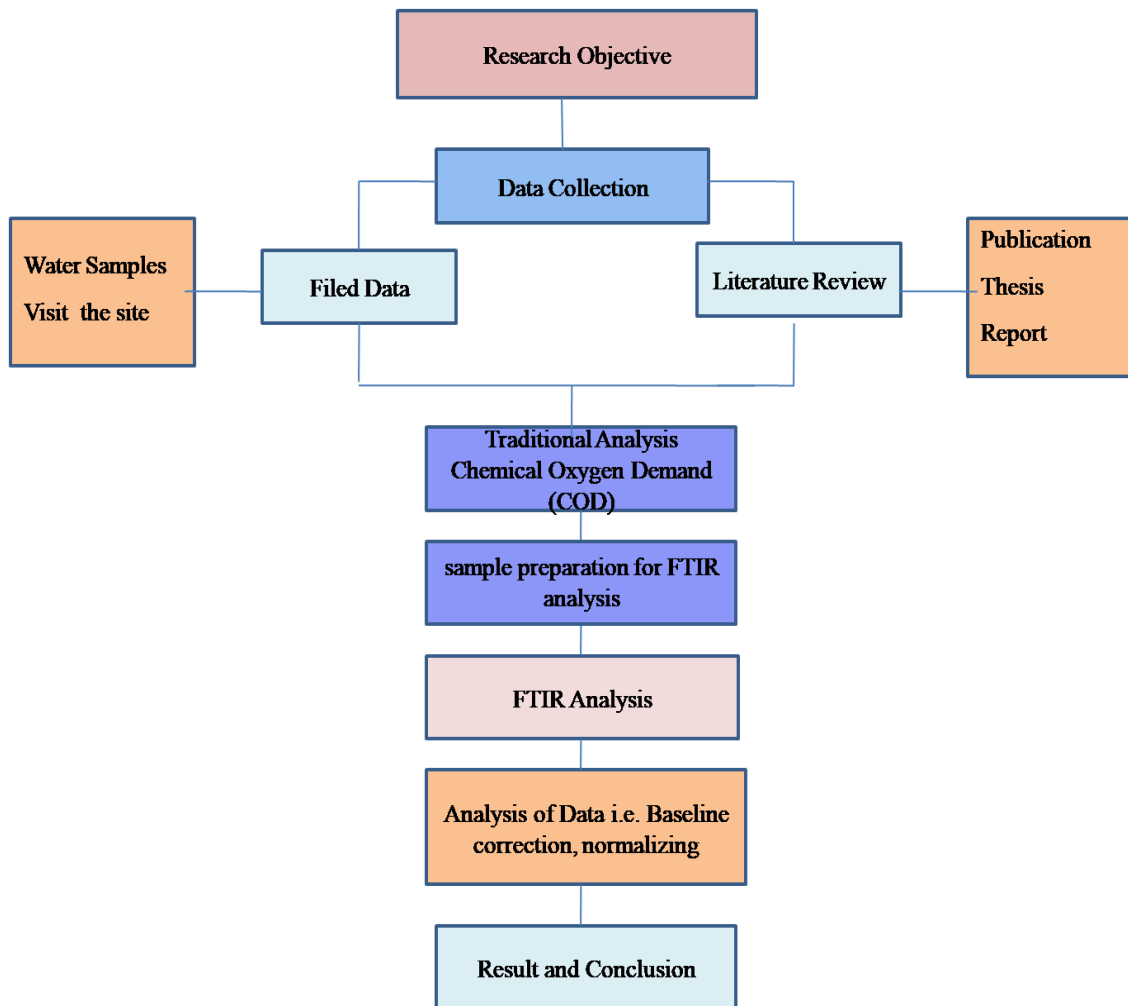


**Figure 4.1:** Research Methodology.

## **4.2 Water Sampling**

### **4.2.1 Sampling Sites**

In collaboration with the Water and Environmental Studies Institute (WESI) of An-Najah National University, sampling sites were selected from three sampling points along Wadi Al-Badan (see Figure 4.2), which are summarized as follows:

Point (1) was selected at wastewater effluent outfall at the eastren part of Nablus at Azmout, Salim junction.

Point (2) was selected at certain distance downstream of point (1) where untreated wastewater are being mixed with Al-Badan fresh springs water close to At-Tawaheen park.

Point (3) was selected at certain distance downstream of point (2) where the untreated wastewater completely mixed with Al-Badan fresh springs water.

### **4.2.2 Sampling Collection**

Second water samples were collected in August 2018 from the three selected points along Wadi Al-Badan. For each site, water sample was collected in a plastic bottle, with a total volume of 3 Liters. All samples were labeled by sampling point numbers, date and time. Afterword, all samples were transferred and stored at WESI laboratory for analysis.

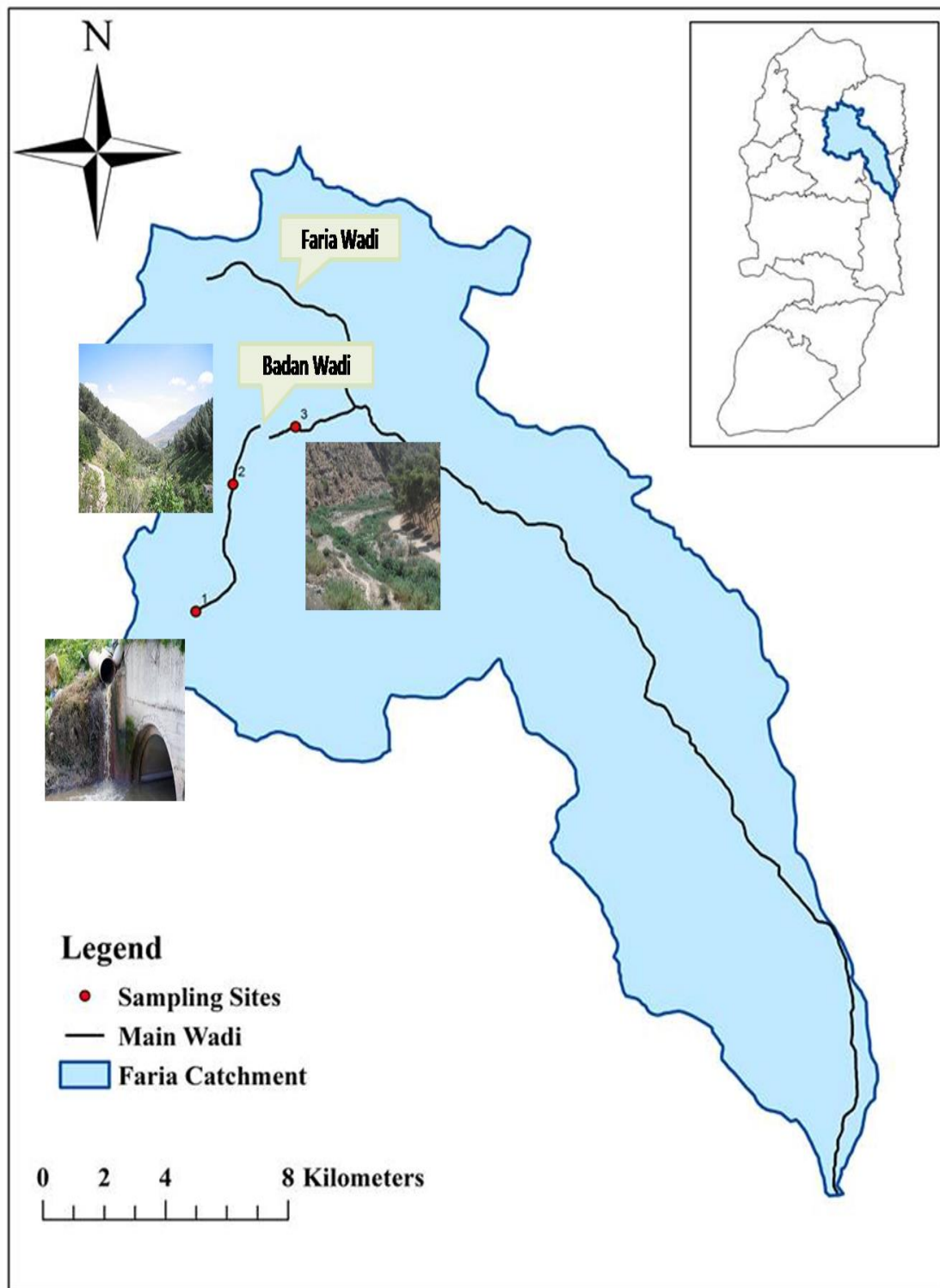
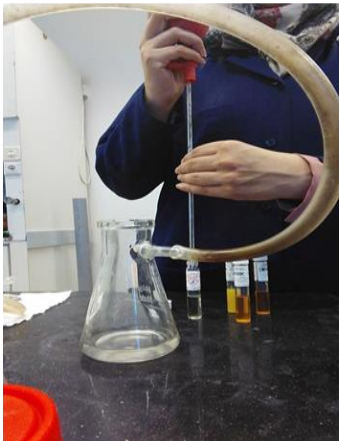


**Figure 4.2:** Location map of selected sampling sites.

### 4.3 Samples Analysis and Preparation

Water samples were analyzed to examine the DOM pollutants using the COD test that is performed according to 5220B Open Reflux method [24]. The COD test was conducted for three samples (See Figure 4.3) as follows:

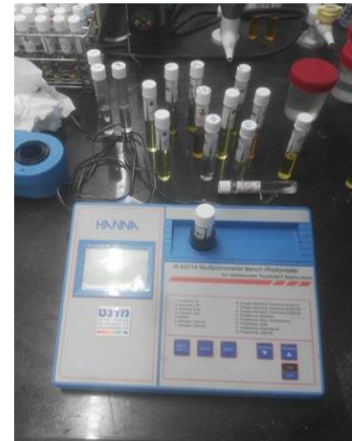
1. All water samples were filtered twice through 450  $\mu\text{m}$  to get DOM.
2. Prepared high range (150 and 1500 ppm) vials are selected for COD testing based on the concentration of DOC in wastewater.
3. 2 ml of wastewater from point (1) was added to 1500 ppm vial and 2 ml of diluted wastewater from point (2) and (3) added to 150 ppm vial and then mixed them well.
4. All vials were placed into the reactor block at a temperature of 150°C for two hours.
5. After two hours, the vials were removed from the block and placed into the colorimeter to read the concentration of COD.



(a)



(b)



(c)

**Figure 4.3:** COD testing preparation: (a) preparation of vials (b) All vials are placed into reactor for two hrs (c) testing the COD concentration by colorimeter.

The strength of wastewater is classified by COD test from weak to strong as following Table 4.1. The results of COD test are summarized in Table 4.2.

**Table 4.1: Wastewater strength in term of COD test [25].**

| <b>Strength</b>    | <b>COD (mg/l)</b> |
|--------------------|-------------------|
| <b>Weak</b>        | <b>&lt;400</b>    |
| <b>Medium</b>      | <b>700</b>        |
| <b>Strong</b>      | <b>1000</b>       |
| <b>Very strong</b> | <b>&gt;1500</b>   |

**Table 4.2: Routine analysis results for COD test.**

| <b>Sampling point</b> | <b>COD (mg/l)</b> | <b>Strength</b> |
|-----------------------|-------------------|-----------------|
| <b>1</b>              | <b>670</b>        | <b>Medium</b>   |
| <b>2</b>              | <b>209</b>        | <b>Weak</b>     |
| <b>3</b>              | <b>128</b>        | <b>Weak</b>     |

After COD test, all water samples were selected for isolation from water to better analyze the DOM structure. The isolation of DOM from water was carried out for the three samples of 3liters each (see Figure 4.4) as follows:

1. All water samples were filtered through 420mm and then 0.45  $\mu\text{m}$  membrane filters (Whatman Co) to extract the suspended matter.
2. An initial volume 3liters for each site was evaporated in two stages, the first stage at 80-85°C in a Heidolph VV 2000 rotary evaporator to volume < 100 mL and the second stage followed by oven drying at 50°C. The obtained suspended solid was studied by FTIR analysis.

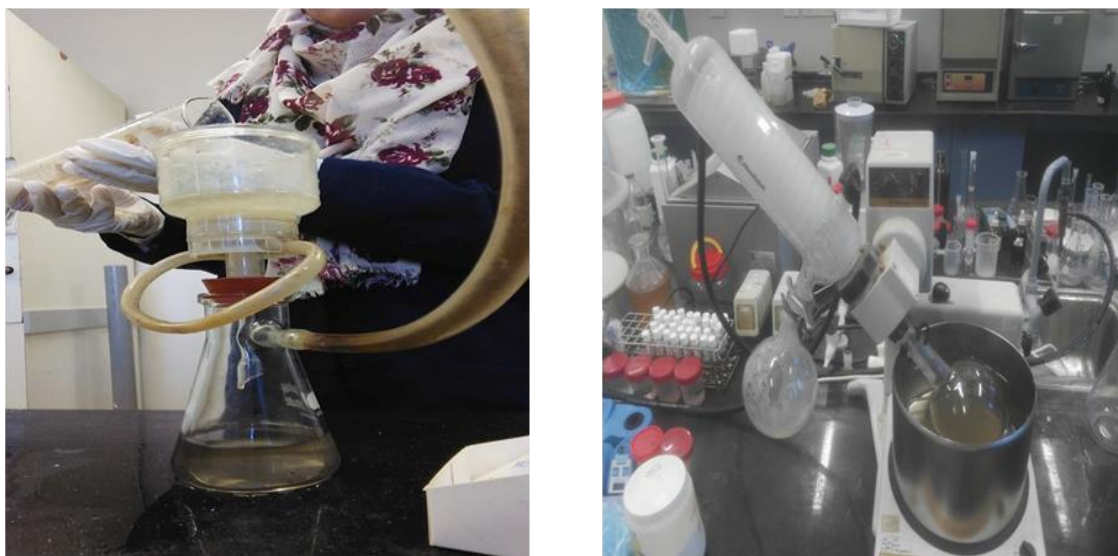


**Figure 4.4:** Solid samples preparation for FTIR analysis: (a) filtering all water samples using paper filter from mm to micrometer to get DOM (b) evaporation the filtered water to get suspended solid.

#### 4.4 FTIR Analysis

The suspended solids were analyzed using Thermo Scientific© Nicolet Continuum IR-microscope with Liquid nitrogen cooled MCT detector which is coupled with the 8700 Thermo Scientific© FTIR spectrometer. The samples were prepared by grounding gently with a mortar and pestle. After that, the samples were subjected into stage of microscope for FTIR scanning. FTIR results were analyzed in terms of diffused reflectance. The final spectrum for each sample was obtained by taking different spectra in different locations in the same sample and then taking the average. The spectral data were calculated by thermal IR source in the mid region range from (4000-400  $\text{cm}^{-1}$ ), spectral resolution of 8  $\text{cm}^{-1}$ , and 46 scans. After spectral measurements, essential FTIR software was used for initial analysis to get highly smooth with lower signal to noise ratio.

**Chapter Five**  
**Chemical Characterization of the Dissolved**  
**Organic Matter**

## **Chapter Five**

### **Chemical Characterization of the Dissolved Organic Matter**

In this research, the composition of DOM compounds is unknown, so the frequency assignments approach are more suitable to use. The general frequency assignments of FTIR spectra for DOM fractions are shown in Table 5.1. The frequency assignments are classified by different functional groups then labeled into several compound classes. The FTIR spectra of all three solid samples are presented in figure 5.1, 5.2, and 5.3. According to Table 5.1, peaks in FTIR spectra for all three solid samples, which are taken from figure 5.1, 5.2, and 5.3, are characterization in terms of peak assignments in table 5.2. Also each peak in FTIR spectra of all samples is described as strong, medium, and weak band, as shown in Table 5.3.

**Table 5.1: General assignments of FTIR spectra of DOM fractions [26] [27].**

| <b>Absorption (cm<sup>-1</sup>)</b> | <b>Peak Assignment</b>                       | <b>Compound class</b>                       |
|-------------------------------------|--|---|
| 3300-3400                           | O-H  | Carboxylic groups                           |
| 3200                                | N-H  | Amide                                       |
| 2800-3000                           | CH <sub>2</sub> , CH <sub>3</sub>            | Alkyl, aliphatic C-H, Alkane                |
| 2500                                | O-H  | Carboxylic groups                           |
| 1735-1700                           | C=O  | Carboxylic groups and carbonyl groups       |
| 1690-1650                           | C=O  | Amide 1                                     |
| 1650-1580                           | C=C, COO <sup>-</sup>                        | Aromatic group, ester                       |
| 1570-1530                           | N-H, C-N                                     | Amide-2                                     |
| 1520-1500                           | C=C, C=N                                     | Lignin, Aromatic group                      |
| 1480-1380                           | , CH <sub>2</sub> , CH <sub>3</sub><br>C-O-H | Aliphatic group,<br>carboxylic acid         |
| 1320-1150                           | C-O, C-O-C                                   | Carboxylic acid, ester, phenols,<br>alcohol |
| 1120-1000                           | C-O, O-H                                     | Carbohydrate, ester, ethers                 |
| 900-650                             | C-H  | Alkynes, aromatic                           |

**Table 5.2: Peak assignments in FTIR spectra of all three solid samples.**

| Absorption ( $cm^{-1}$ ) |          |         | Peak Assignment                              | Compound Class                       |
|--------------------------|----------|---------|--|--------------------------------------|
| Sample 1                 | Sample 2 | Sample3 |  |                                      |
| 3269                     | 3358     | 3342    | O-H  | Carboxylic acid ,alcohol             |
| 2959                     | 2953     | 2964    | C-H  | Alkyl, aliphatic C-H, Alkane         |
| 2525                     | 2741     | 2658    | O-H  | Carboxylic acid                      |
| -                        | 1718     | 1792    | C=O  | Carbonyl group and carboxylic group  |
| 1588                     | 1624     | 1620    | C=C,C=O                                      | Amide-1 , aromatic group             |
| 1433                     | 1470     | 1460    | CH <sub>2</sub> , CH <sub>3</sub> ,<br>C=O-H | Aliphatic group, carboxylic acid     |
| 1099                     | 1083     | 1083    | C-O, C-O-C,<br>O-H                           | Carbohydrate, ester, phenol, alcohol |
| 863                      | 891      | 879     | C-H  | Alkynes, aromatic                    |
| 785-715                  | 746-686  | 739-679 | C-Cl   | Chlorocompound                       |

**Table 5.3: Peak intensities in FTIR spectra of all three solid samples.**

| Samples and Peak Assignment ( $cm^{-1}$ ) | Sample 1      | Sample 2      | Sample 3      |
|---|---------------|---------------|---------------|
| Hydroxyl (3000-3600)                      | Strong, Broad | Strong, Broad | Strong, Broad |
| Carbonyl (1710-1850)                      | -             | Weak          | Weak          |
| Aromatic (1620-1580)                      | Strong        | Medium        | Medium        |
| Aliphatic (1380-1480)                     | Strong        | Medium        | Medium        |
| Carbohydrate (1000-1200)                  | Medium, Broad | Strong, Broad | Strong, Broad |

## 5.1 Chemical Characterization of Dissolved Organic Matter in the Solid Samples

Solid obtained from sampling point 1 (raw wastewater) has been analyzed by FTIR analysis for DOM chemical compounds in term of functional groups. The FTIR spectra of sample 1 are presented in Figure 5.1. Table 5.2 lists all absorbance peaks and bands present in the FTIR average spectrum. In higher frequency, FTIR average spectrum is characterized by a strong broad spectral band in the range from  $3000\text{cm}^{-1}$  to  $3600\text{cm}^{-1}$ , which results from (O-H) stretching vibration band of hydrogen-bonded hydroxyl functional group in alcohol and carboxylic acid, as well as (N-H) group in amides. In addition to Small band appears on the left side of broad band with maximum absorption at  $2947\text{ cm}^{-1}$ , which is assigned to (C-H) asymmetric and symmetric stretching vibrations band in aliphatic compounds [28]. The strong intensity bands observed at  $1588\text{ cm}^{-1}$  and  $1433\text{ cm}^{-1}$ , which are assigned to the aromatic (C=C) vibration and bending of (C-H) band in aliphatic compounds, respectively.

There is a band at around  $1100\text{cm}^{-1}$ , which is generally related to (C-O) asymmetric stretching of carbohydrates, such as polysaccharide or long chain fatty acids or phenol [29]. When comes to lower frequency, sharp peaks at around  $700\text{-}800\text{cm}^{-1}$  are assigned to C-Cl stretching in alkyl halides.

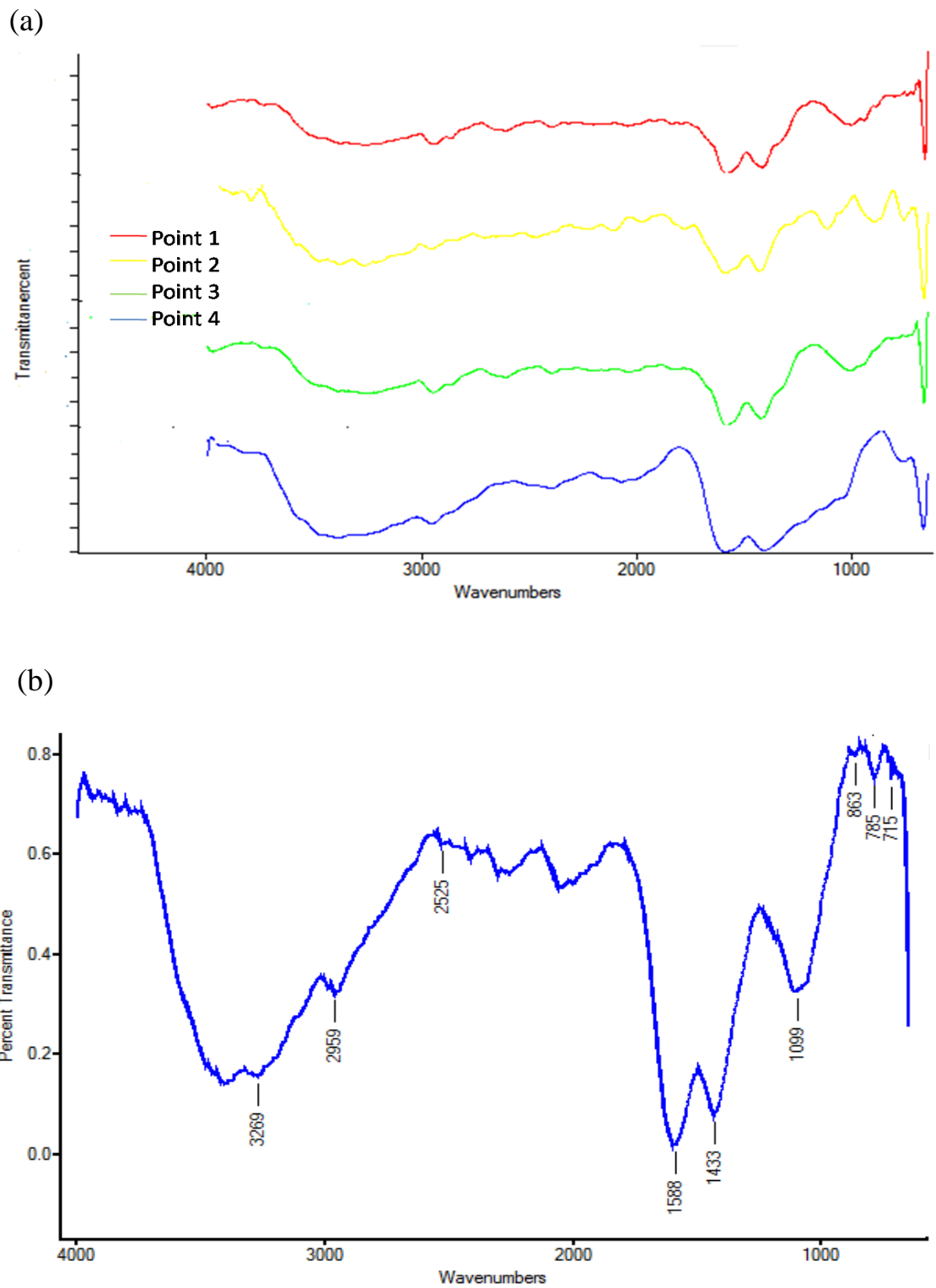


**Figure 5.1:** FTIR spectra of sample (1): (a) FTIR spectra of four points in the sample, (b) average spectrum of four points.

FTIR spectra of sample 2 collected from point (2) are shown in Figure 5.2. By comparing the FTIR spectra of samples 1 and 2, the two spectra are very similar to each other in the position and shape of the absorption bands at higher frequency, but they have some difference in position and intensity of the main absorption bands in the region below  $1800\text{ cm}^{-1}$ .

In the region below  $1800\text{ cm}^{-1}$  of the spectrum of sample 2, a medium intensity band observed at  $1624\text{ cm}^{-1}$ , which are assigned to (C=O) stretching vibration of amide1, (C=C) stretching vibration of aromatic. There is a weak and small peak around  $1516\text{ cm}^{-1}$  might be assigned to (N-H) bending vibration band or (C-N) stretching vibrations band in amide-2, while peak at around  $1470\text{ cm}^{-1}$  is related to aliphatic C-H deformation in alkane. One of the most apparent waveband is a strong and broad peak observed at  $1083\text{ cm}^{-1}$  resulting from (C-O) asymmetric stretching of carbohydrates, such as polysaccharides or aromatic ethers [30]. In lower frequency, the spectrum is characterized by sharp peaks at around  $891\text{ cm}^{-1}$  which is related to C-H bending in aromatic vibration or alkenes, while the peaks at around  $700\text{-}780\text{ cm}^{-1}$  are assigned to C-Cl stretching in alkyl.

Compared with sample1, sample 2 has smaller peak at around  $1470\text{ cm}^{-1}$ , indicating a decrease of aliphatic compounds along the Wadi. Additionally, there is a stronger and abroad peak at  $1083\text{ cm}^{-1}$  instead of medium band, indicating an increase in ester and acid.

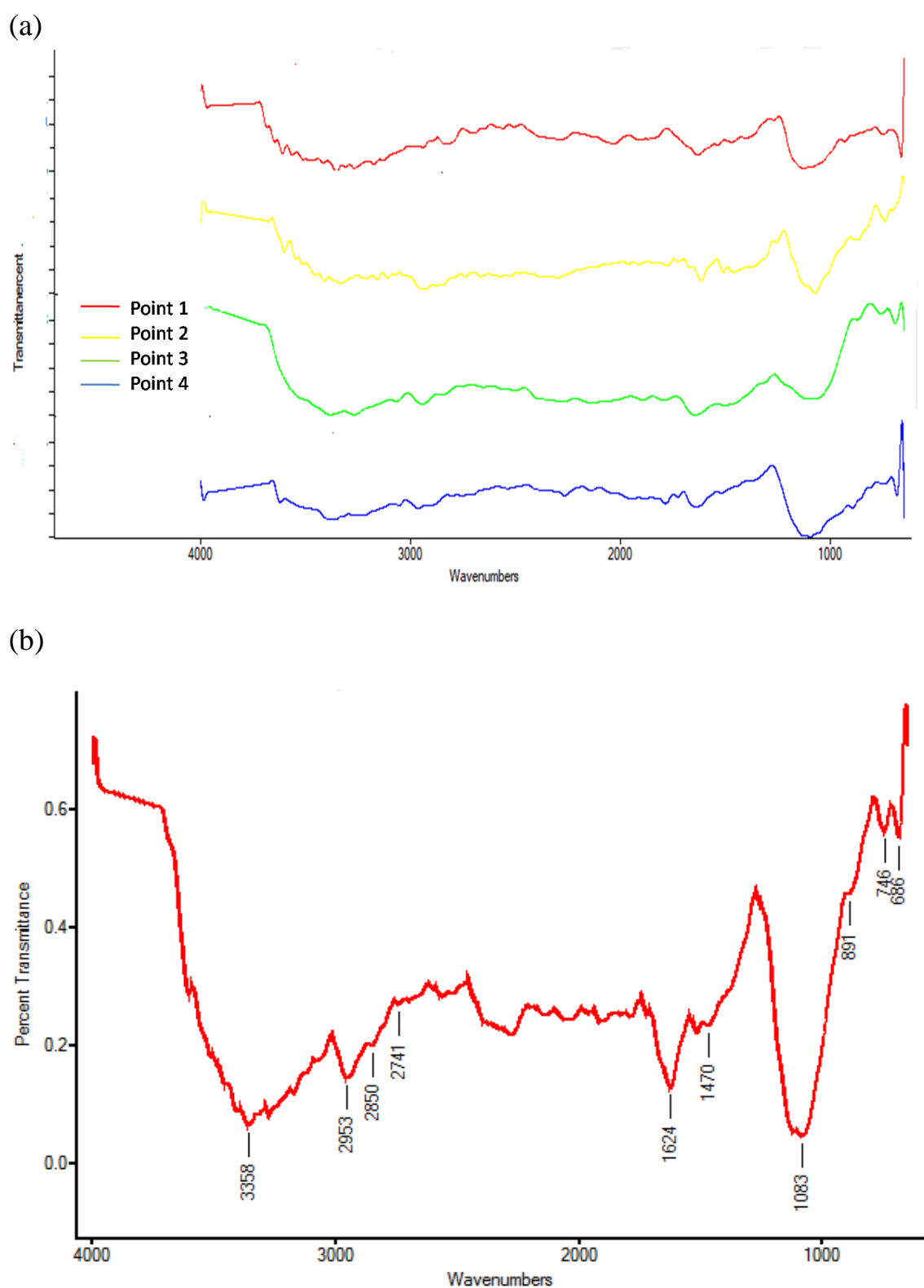
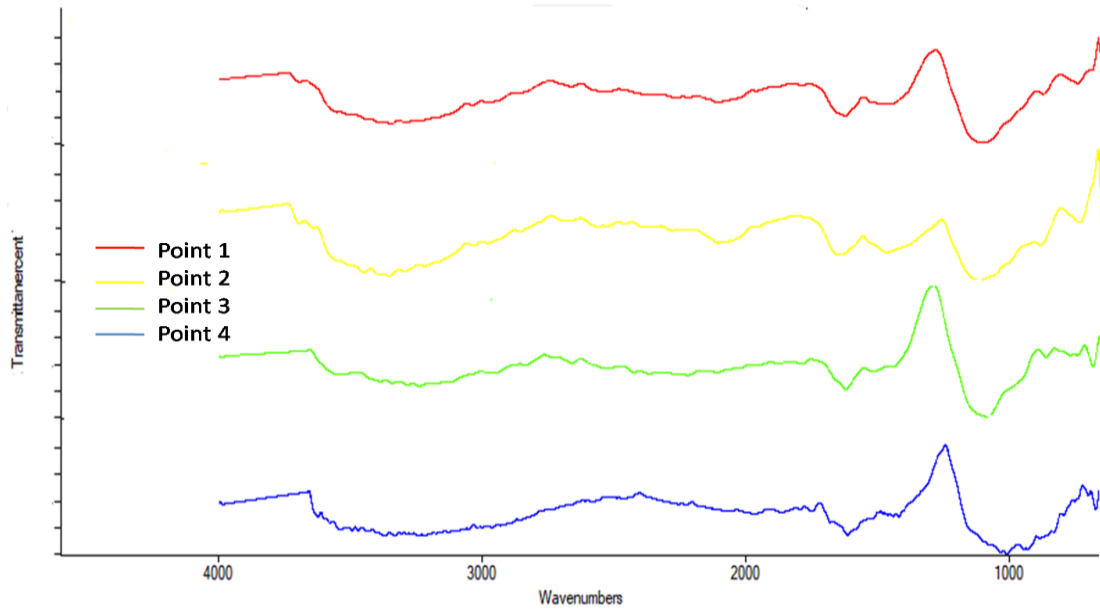


**Figure 5.2:** FTIR spectra of sample (2): (a) FTIR spectra of four points in the sample, (b) average spectrum of four points.

FTIR spectra of sample 3 collected from point (3) are shown in Figure 5.3.

(a)



(b)

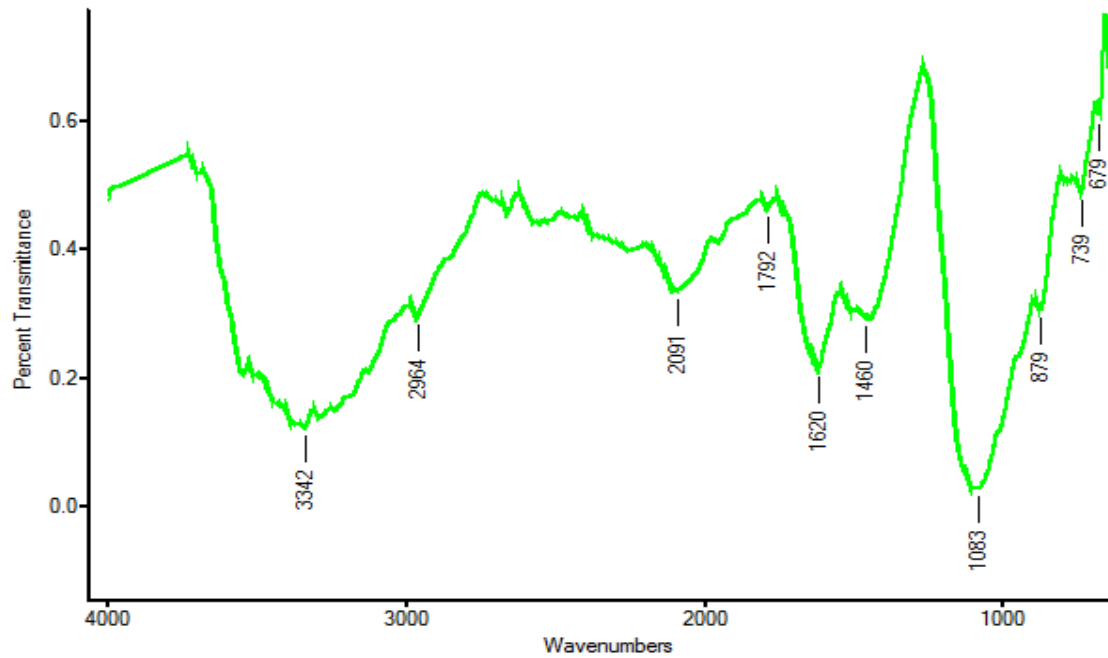


**Figure 5.3:** FTIR spectra of sample (3): (a) FTIR spectra of four points in the sample, (b) average spectrum of four points.

By comparing the FTIR spectra of samples 2 and 3, two spectra are very similar to each at higher frequency, but they have some different in the region below  $1800\text{cm}^{-1}$ .

In the region below  $1800\text{ cm}^{-1}$ , weak peaks at around  $1718\text{-}1738\text{ cm}^{-1}$  appear in sample 3 while sharper and stronger appear in sample 2, indicating a lower concentration of carboxylic acids or ether.

FTIR spectra for all three solid samples are shown in Figure 5.4. Sample 1 collected from outfall system has some largest absorption bands which suggest the outfall has the highest DOM concentration.

The change of the DOM concentration along wadi Al-Badan indicates by decrease or increase in peak response measures in absorbance unit on y-axis. Comparison of the absorption response of three FTIR spectra of three samples indicates that the aromatic and aliphatic functional groups decrease along the Wadi, while stretching vibration of (C-O) band increase along the Wadi.

In Conclusion, DOM in all three samples along the Wadi stream flow showed a decrease in aromatic and aliphatic functional groups and increasing of (C-O) containing compounds as well as carbohydrates and carboxylic acid. Moreover, samples from same point source (along wadi Al-Badan) are very similar to each other in the position and shape of the absorption bands in FTIR spectra, but their absorption bands have some difference in the intensity due to the effects of DOM input from surroundings or natural purification.

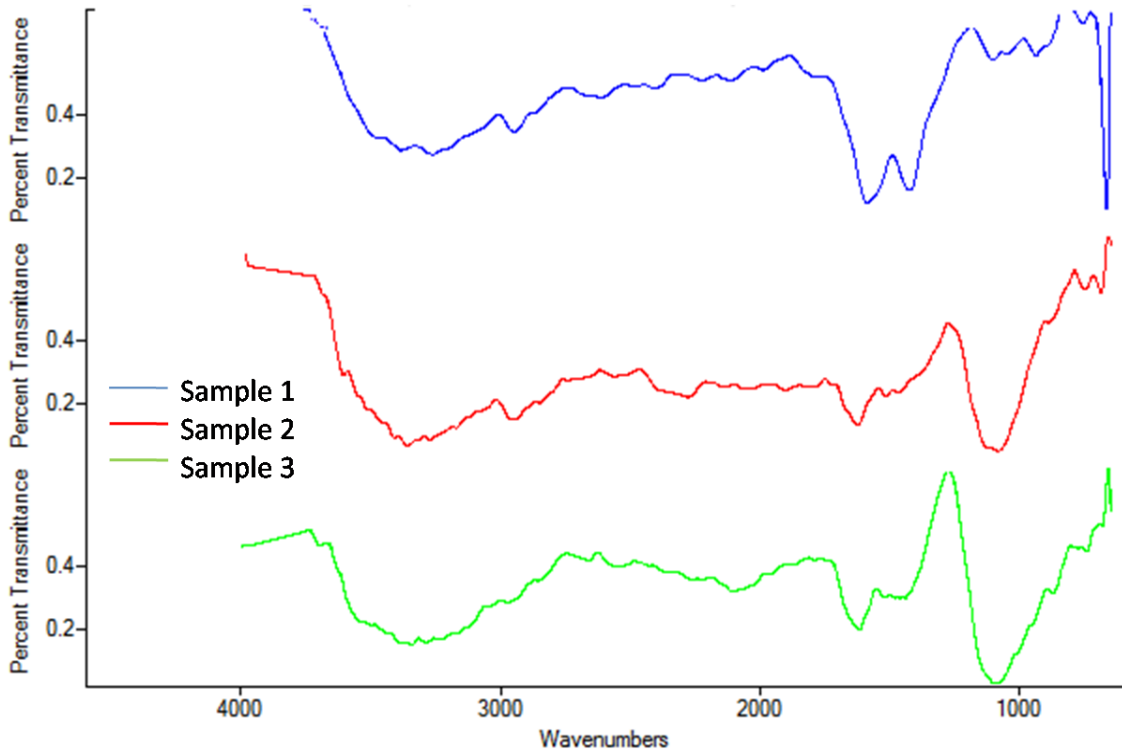


**Figure 5.4:** FTIR spectra of all three solid samples from different points along wadi Al-Badan: sample1 from point 1, sample 2 from point 2, sample 3 from point 3.

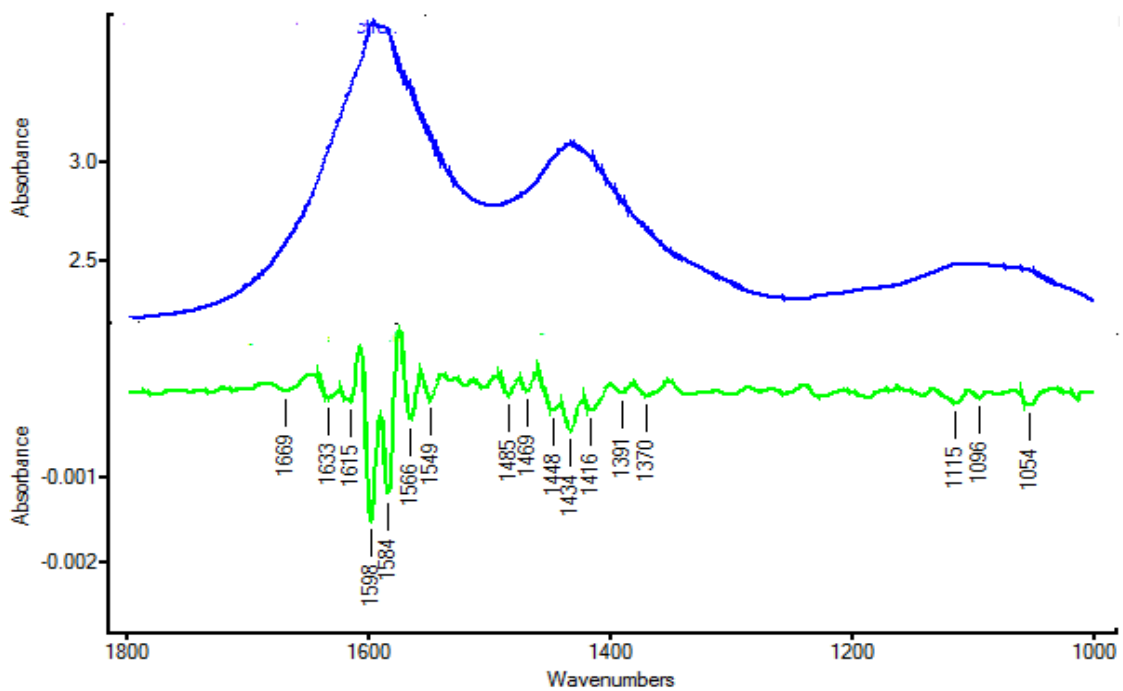
## 5.2 Identification More Important Chemical Compounds

DOM components are complex and each component is composed of multiple bands, so they overlap with each other and form unstructured bands. Derivation of FTIR spectra allows separating overlapping of bands and identifying some bands that are hidden under the broad band [28]. The second derivative spectra for all three solid samples have been calculated as shown in Figure 5.5 for overlapped area in the range from  $1000\text{ cm}^{-1}$  to  $1800\text{ cm}^{-1}$ , indicating the vibration bands for carboxylic acid, amides, ester, and carbohydrate. The full list of all resolved peaks and their assignments are shown in table 5.4. From the peak assignments shown in table 5.4, Carboxylic acid (COOH) and Aliphatic ester peaks are largely

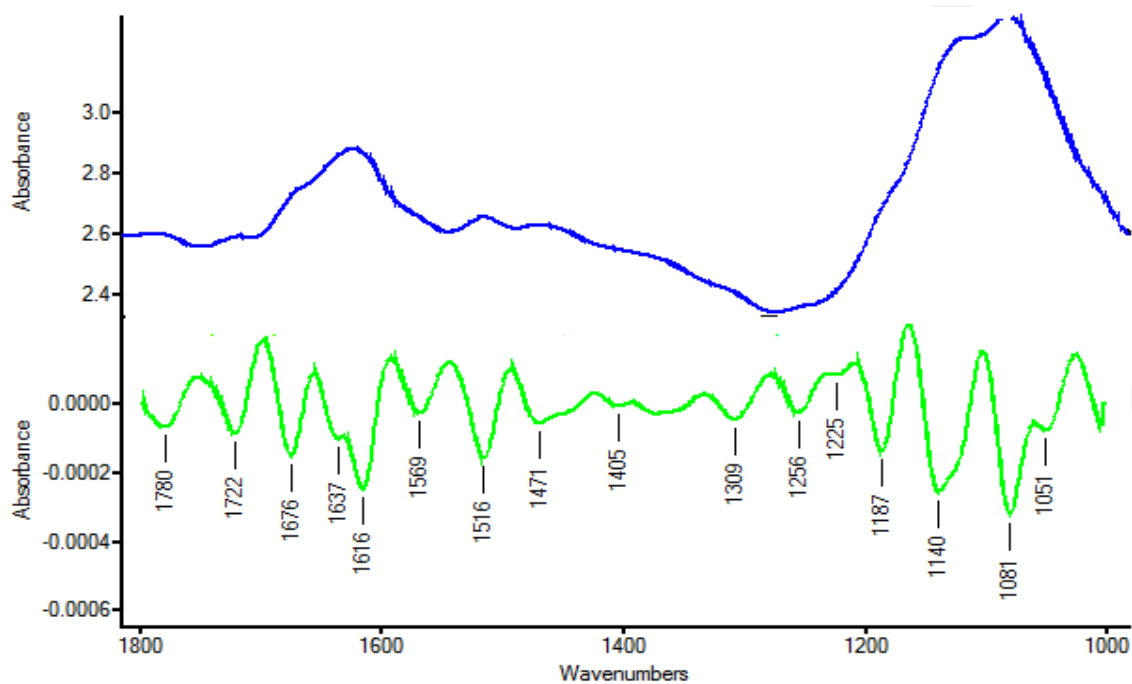
present in sample 2 and 3, indicating an increase of carboxylic acid and aliphatic ester along the wadi. As for amides, (C=O) and (N-H) peaks are identified in order to indicate the distribution of amide 1 and amide 2, respectively. (C=O) stretching peaks are largely existing in all samples in the range from 1630-1680  $\text{cm}^{-1}$  while the (N-H) bending peaks decrease sharply along the Wadi. When it comes to carbohydrate, there are many bands in the range (1200-1000  $\text{cm}^{-1}$ ) in samples 2 and 3, indicating carbohydrate largely exist in point 2 and 3.

As for alkane compound, the alkane peaks (with typical aliphatic functional group) in the range 1360-1480  $\text{cm}^{-1}$  are largely exist in sample 1 then the peaks decrease in sample 2 and 3, indicating decrease of alkanes compound along the Wadi.

(a)



(b)



(c)

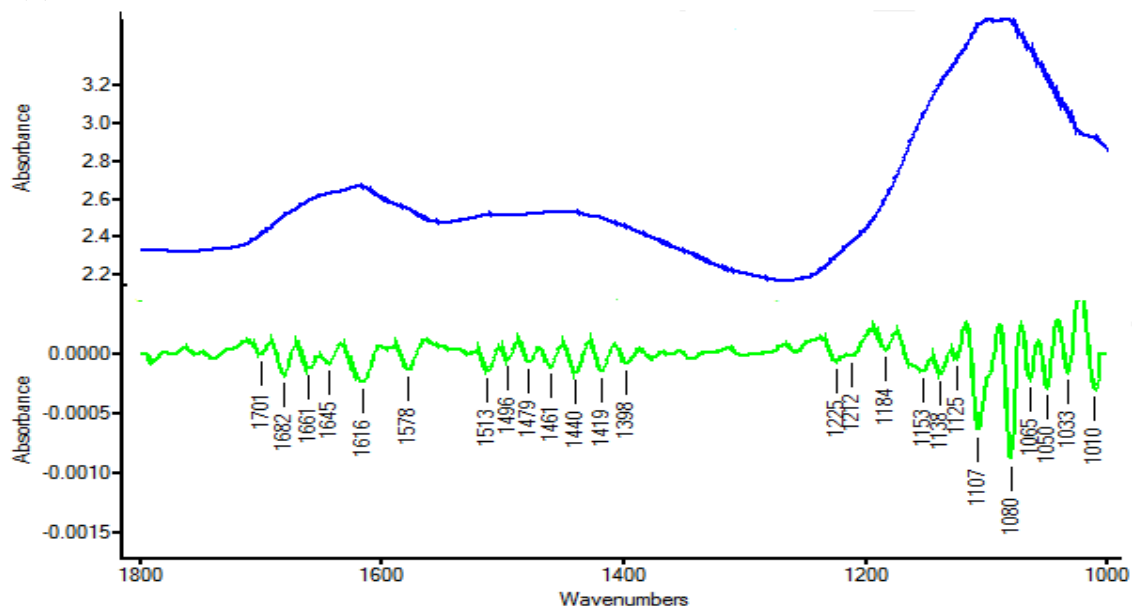


**Figure 5.5:** FTIR spectra (blue line) and secondary derivative (green line) of the solid samples in the range 1000-1800  $\text{cm}^{-1}$  from different points along Wadi Al-Badan: (a) Sample 1 from point1, (b) sample 2 from point 2, (c) sample 3 from point 3.

**Table 5.4: Peak assignments and positions of each compound class in secondary derivative FTIR spectra of all three solid samples.**

| Compound classes | Peak Assignment (cm <sup>-1</sup> )              | Band position in samples |                              |                                      |
|------------------|--|--------------------------|------------------------------|--------------------------------------|
|                  |  | Sample 1                 | Sample 2                     | Sample 3                             |
| Carboxylic acid  | C=O(stretch:1730-1700)                           | No                       | 1722                         | 1701                                 |
|                  | C-O(stretch:1320-1210)                           | 1220                     | 1225<br>1256                 | 1212<br>1225                         |
|                  | O-H (bend in-plan: 1440-1395)                    | 1436                     | 1426                         | 1409                                 |
| Amide            | Amide1(C=O stretch: 1680-1630)                   | 1633<br>1669             | 1637<br>1676                 | 1645<br>1661                         |
|                  | Amide2 (N-H bend: 1550-1570)                     | 1550<br>1566             | 1569                         | No                                   |
| Aliphatic Ester  | C=O(stretch:1750-1730)                           | No                       | No                           | 1732                                 |
|                  | C-C-O(stretch:1200-1160)                         | No                       | 1187                         | 1184                                 |
|                  | O-C-C(stretch:1100-1030)                         | 1054<br>1096             | 1051<br>1081                 | 1060<br>1065<br>1080                 |
| Carbohydrate     | C-O( asymmetric stretch:1200-1000)               | 1054<br>1096<br>1115     | 1051<br>1081<br>1140<br>1187 | 1010<br>1033<br>1060<br>1065<br>1080 |
|                  | O-H (bend:1400-1300)                             | No                       | 1309                         | 1398                                 |
| Alkane           | CH <sub>2</sub> deformation:1480-1440            | 1448<br>1469             | 1471                         | 1440<br>1461                         |
|                  | CH <sub>3</sub> symmetric deformation :1390-1365 | 1370<br>1391             | No                           | No                                   |

## 5.3 Discussion

### 5.3.1 Chemical Characterization of Dissolved Organic Matter in all Solid Samples

All three samples collected along wadi Al-Badan were analyzed by diffuse reflectance FTIR microspectroscopy. Absorption bands were identified for each sample. After that, similarities and difference were compared between the samples. Secondary derivative was used in the second stages to identify some peaks that were hidden under broad bands. In this section, the features of DOM are discussed in all three samples.

In the FTIR spectra of these three samples, the intensity of (C-H) band at around 1380-1480  $\text{cm}^{-1}$ , likely from alkane, decreases sharply along the Wadi, while the (C-O) band at around 1000-1200  $\text{cm}^{-1}$  increases along the Wadi. From secondary derivative spectra, the distributions of amide-1 are explored in each sample while distribution of amide-2 finds only in sample 1 and 2. As for carboxylic acid and aliphatic ester, they are largely present in sample 2 and 3.

In conclusion, the three samples along the wadi Al-Badan shows a decreasing of aliphatic and aromatic groups and increasing of (C-O) band contains component as well as carbohydrate or aromatic ether. In addition to the FTIR spectra of the three samples from the same point source have similar basic shape, but are different in the intensity of some specific bands.

### 5.3.2 Chemical Characterization of Dissolved Organic Matter from the Same Point Source

All three samples collected along wadi Al-Badan are contaminated with untreated wastewater. Wastewater is considering the main point pollution source in this study. Urban wastewater is a mixture of domestic, industrial wastewater together with run-off rain, which contains several pollutants like organic matter. In this section, the peaks of DOM from same point sources will be discussed and explored the interaction between DOM and its surroundings.

From the FTIR spectra of all three samples, the most obvious observation bands are at around  $1588\text{ cm}^{-1}$  and  $1433\text{ cm}^{-1}$ , indicating high concentration of aromatic and aliphatic compounds in sample 1, respectively. In the range  $1000\text{-}1800\text{ cm}^{-1}$ , we take advantages of secondary derivative spectra in figure 4.5 to overlap area. In the region of  $1000\text{-}1200\text{ cm}^{-1}$  multi intense band only appear in the sample 2 and 3, which implies large amount of carbohydrate. In the region  $1580\text{-}1620\text{ cm}^{-1}$ , multi intense peaks only appear in sample 1, indicating a large amount of aromatic. Amides observe at around  $1650\text{ cm}^{-1}$  and  $1550\text{ cm}^{-1}$  become visible in each spectrum. In the region  $1700\text{-}1750\text{ cm}^{-1}$ , multi bands only appear in sample 1 and 2, indicating large amount of carboxylic acid and ester.

From the result we obtained, the carbohydrate and carbonyl groups increased in sample 2, indicating that wadi Al-Badan was affected by not only untreated wastewater but other non-point pollution sources as well. Leaching of plant leaf and organic matter rich soils which come from forest area always contains carbohydrate and some of them drained into wadi [31].

## Chapter Six

### Conclusions and Recommendations

#### 6.1 Conclusions

The Selected water samples along Wadi Al-Badan were analyzed for DOM using two different methods: traditional and FTIR methods. Comparing the two techniques, FTIR has the advantage that can directly provide overview of chemical compositions for each sample and information about interaction between DOM and surroundings. Traditional analysis is helpful to assess the presence DOM in the selected water samples. During FTIR analysis, DOM for each sample is identified. With the information carried by DOM features in samples, the relationship between DOM and surroundings is observed. The main conclusions about DOM analysis are described as follows:

1. The result shows that the major chemical compounds in selected water samples are: Aliphatic, aromatic, amide and carbohydrate.
2. The result shows that samples from the same point pollution source has similar characteristics within the group, but are different in the concentrations.
3. The result shows that carbohydrate and carbonyl components have increase along the Wadi which shows that wadi Al-Badan is affected with the nonpoint pollution sources from surroundings.
4. The result shows aliphatic and amide-2 have decrease slightly along the Wadi which is affected by natural purification or human activities.

## 6.2 Future recommendations

The study presents important recommendations for future work:

- One important recommendation for future work is continue trying to solve water absorption IR problem. FTIR method has problem with water because water absorb most of IR light and prevents sufficient light from reaching the sample to give a good signal. If this problem is resolved, then live cell in aqueous solution can be study and this will make revolution in FTIR application. In addition, the used of synchrotron light provides great biochemical detailed over traditional sources.
- It is also recommended to collect water samples in different seasons. The water samples in this research were taken in the summer. Therefore, The DOM characteristics were only represented during the summer. Because the DOM characteristics are likely to change seasonally, these variations should be investigated in future study. It is also recommended to take water samples from wastewater treatment to evaluate of wastewater treatment processes.

## References

- (1) Al-Khatib and S. Salah (2003). "*Bacteriological and chemical quality of swimming pools water in developing countries: a case study in the west bank of Palestine*". **International Journal of Environmental Research**, Volume 13, Issue 1: Pages (17-22).
- (2) S. Shadeed, et al (2016). "*Assessment of Groundwater in the Faria Catchment*". **An - Najah Univ. J. Res. (N. Sc.)**, Volume 30, Issue 1.
- (3) T. G. Reyes and J. M. Crisosto (2016). "*Characterization of Dissolved Organic Matter in River Water by Conventional Methods and Direct Sample Analysis-Time of Flight-Mass Spectrometry*". **Journal of Chemistry**, Volume 2016.  
<http://dx.doi.org/10.1155/2016/1537370>
- (4) Man-hong Huang, et al (2010). "*Chemical composition of organic matters in domestic wastewater*". **Desalination**, Volume 262, Issues (1-3): Pages (36-42).
- (5) S. Shadeed, et al (2011). "*Overview of Quantity and Quality of Water Resources in the Faria Catchment, Palestine*". **International Graduate Conference on Science, Humanities and Engineering**. An-Najah National University, Nablus, Palestine.
- (6) L. Bu, et al (2010). "*Characterization of dissolved organic matter during landfill leachate treatment by sequencing batch reactor, aeration corrosive cell-Fenton, and granular activated carbon in series*". **Journal of Hazardous Materials**, Volume 179, Issues (1-3) : Pages (1096-1105).
- (7) F. R. Elder, et al (1947). "*Radiation from Electrons in a Synchrotron*". **Phys. Rev**, Volume 71, Issue 11.

- (8) G. M. Hettiarachchi, et al (2017). *"Application of Synchrotron Radiation-based Methods for Environmental Biogeochemistry: Introduction to the Special Section"*. **Journal of Environmental Quality**, Volume 46, Issue 6: Pages (1139-1145).
- (9) D. Einfeld, et al (2004). *"SESAME, a third generation synchrotron light source for the Middle East region"*. **Radiation Physics and Chemistry**, Volume 71: Pages (693-700).
- (10) **"Yellow book, Conceptual Design Report for the Upgrading of SESAME to 2.5GeV (2003)"**. SESAME Office, Jordan.
- (11) SESAME website: [www.sesame.org.jo](http://www.sesame.org.jo).
- (12) D. Einfeld, et al (2002). *"The New Upgrade of SESAME"*. **Proceedings of EPAC**, Paris, France.
- (13) I. Yousef, et al (2012). *"Simulation and design of an infrared beamline for SESAME (Synchrotron-Light for Experimental Science and Applications in the Middle East)"*. **Nuclear Instruments and Methods in Physics Research A**, Volume 673: Pages (73–81).
- (14) G. Reich (2016). **"Mid and Near Infrared Spectroscopy."** Analytical Techniques in the Pharmaceutical Science. Advances in Delivery Science and Technology. Springer, New York.
- (15) B. H. Stuart (2004). **"Infrared Spectroscopy: Fundamentals and Applications."** Analytical Techniques in the Sciences. Wiley, New York.
- (16) A. A. Christy, et al (2001). **"Modern Fourier Transform Infrared Spectroscopy"**. Elsevier, New York.

- (17) M. Miller and P. Dumas (2006). "*Chemical imaging of biological tissue with synchrotron infrared light*". **Biochimica et Biophysica Acta (BBA) - Biomembranes**, Volume 1758, Issue 7: Pages (846-857).
- (18) B. C. Smith (1996). "**Fundamentals of Fourier Transform Infrared Spectroscopy**". Boca Raton FL, CRC press.
- (19) P. Bassan, et al (2009). "*Reflection contributions to the dispersion artefact in FTIR spectra of single biological cells*". **The Analyst**, Volume 134, Issue 6: Pages (1171-5).
- (20) R. Spragg (2013). "*Reflection Measurements in IR Spectroscopy*". **PerkinElmer, Inc. Waltham, MA**.
- (21) M. A. Farrukh (2012). "**Advanced Aspects of Spectroscopy**". Rijeka, InTech.
- (22) Lu (2013). "**Infrared microscopy applications**". GIA, New York.
- (23) H. Sreedhar, et al (2015). "*High-definition Fourier Transform Infrared (FT-IR) Spectroscopic Imaging of Human Tissue Sections towards Improving Pathology*". **Journal of Visualized Experiments**, Volume 95: Pages (1-10).
- (24) APHA, et al (2005). "**Standard Methods for the Examination of Water & Wastewater**". Twentieth edition, American Public Health Association, Washington, DC.
- (25) Duncan Mara (2004). "**Domestic waste water treatment in developing Countries**". Earth-scan112, UK.
- (26) A. Tinti, et al (2015). "*Recent applications of vibrational mid-Infrared (IR) spectroscopy for studying soil components: a review*". **Journal of Central European Agriculture**, Volume 16, Issue 1: Pages (1-22).

- (27) E. Minor and B. Stephens (2008). "***Dissolved organic matter characteristics within the Lake Superior watershed***". **Organic Geochemistry**, Volume 39, Issue 11: Pages (1489-1501).
- (28) S. Mazurek, et al (2013). "***Transmission Fourier transform infrared microspectroscopy allows simultaneous assessment of cutin and cell-wall polysaccharides of Arabidopsis petals***". **The Plant Journal**, Volume 74, Issue 5: Pages (880–891).
- (29) B. M. Stephens and E. C. Minor (2010). "***DOM characteristics along the continuum from river to receiving basin: A comparison of freshwater and saline transects***". **Aquatic Sciences**, Volume 72, Issue 4: Pages (403-417).
- (30) S. Yusuf and A. A. Audu, et al (2017). "***Characterization of dissolved organic matter in selected wetlands from northern Nigeria***". **FUW Trends in Science & Technology Journal**, Volume 2, Issue 1: Pages (227-238).
- (31) S. ZHANG (2015). "**Characterization of dissolved organic matter in water using Fourier Transform Infrared spectroscopy and X-ray photoelectron spectroscopy: Implication for chemical composition and effects of water sources.**" MS Thesis, the University of Missouri-Columbia.

توصيف المادة العضوية الذائبة في وادي البادان  
باستخدام مجهر فورييه للتحويل بالأشعة تحت  
الحمراء في سيزمي

اعداد

امل عطاري

باشراف

د. احمد بصلات

د. سمير شديد

قدمت هذه الأطروحة استكمالاً لمتطلبات الحصول على درجة الماجستير في الفيزياء بكلية الدراسات  
العليا في جامعة النجاح الوطنية في نابلس، فلسطين

2019

ب

توصيف المادة العضوية الذائبة في وادي البادان باستخدام مجهر فورييه للتحويل بالأشعة تحت

الحمراء في سيزمي

اعداد

امل عطارى

باشراف

د. احمد بصلات

د. سمير شديد

## الملخص

وادي البادان هو أحد روافد حوض الفارعة الذي يبدأ جريانه من الأجزاء الشرقية لمدينة نابلس. تدهورت جودة المياه في الوادي بسبب التلوث الناتج عن التدفق المستمر للمياه العادمة الغير المعالجة من شرق مدينة نابلس. المياه العادمة تحتوي على المواد العضوية الذائبة (DOM) والتي بدورها يمكن ان تنشط نمو الكائنات الحية الدقيقة في مياه الوادي. وجود الملوثات الميكروبيولوجية يمكن أن تلوث موارد المياه السطحية والجوفية في حوض الفارعة وهذا سوف يعرض المستهلكين المحليين للخطر وبشكل رئيسي أولئك الذين يستخدمون المياه لأغراض الشرب. لذلك، من المهم دراسة وتوصيف DOM في وادي البادان. تم جمع عينات ممثلة لمياه الوادي وتحليلها باستخدام طريقتين: أولاً ، باستخدام التحليل التقليدي الذي أجري في مختبرات معهد الدراسات المائية والبيئية (WESI) في جامعة النجاح الوطنية وثانياً باستخدام تحليل FTIR في ضوء السنكروترون للعلوم والتطبيقات التجريبية (SESAME) في الأردن. لتحليل FTIR، بعد الحصول على أطياف DOM، تم تحليلها باستخدام برنامج Essential FTIR، الذي يسمح بتحديد قمم مختلفة لمكونات DOM. أظهرت نتائج FTIR أن التواجد الكبير للمركبات المختلفة لـ DOM هي: أميد، مركبات عطرية، أليفاتية، وكربوهيدرات. بالإضافة إلى ذلك، تتأثر المركبات الكيميائية لـ DOM بمدخلات من البيئة المحيطة والتلوث الطبيعية التي تحدث على طول الوادي الرئيسي. أوضحت الدراسة أنه يمكن استخدام طريقة FTIR لتوصيف DOM في النظام المائي وكذلك لتتبع المصادر المحتملة لـ DOM في مياه الوادي.